



## Sequential purification and characterization of *Torpedo californica* nAChR-DC supplemented with CHS for high-resolution crystallization studies

Rafael Maldonado-Hernández<sup>a,c</sup>, Orestes Quesada<sup>b,c</sup>, José O. Colón-Sáez<sup>d</sup>,  
José A. Lasalde-Dominicci<sup>a,c,e,\*</sup>

<sup>a</sup> Department of the Biology, University of Puerto Rico, Río Piedras Campus, San Juan, Puerto Rico

<sup>b</sup> Department of Physical Sciences, University of Puerto Rico, Río Piedras Campus, San Juan, Puerto Rico

<sup>c</sup> Molecular Sciences Research Center, University of Puerto Rico, San Juan, Puerto Rico

<sup>d</sup> Pharmaceutical Sciences, University of Puerto Rico Medical Science Campus, Puerto Rico

<sup>e</sup> Institute of Neurobiology, University of Puerto Rico Medical Science Campus, Puerto Rico

### ARTICLE INFO

#### Keywords:

*Torpedo californica*  
nAChR  
Detergent complexes  
Cholesteryl hemisuccinate  
Circular dichroism  
Two-electrode voltage clamp

### ABSTRACT

Over the past 10 years we have been developing a multi-attribute analytical platform that allows for the preparation of milligram amounts of functional, high-pure, and stable *Torpedo* (muscle-type) nAChR detergent complexes for crystallization purpose. In the present work, we have been able to significantly improve and optimize the purity and yield of nicotinic acetylcholine receptors in detergent complexes (nAChR-DC) without compromising stability and functionality. We implemented new methods in the process, such as analysis and rapid production of samples for future crystallization preparations. Native nAChR was extracted from the electric organ of *Torpedo californica* using the lipid-like detergent LysoFos Choline 16 (LFC-16), followed by three consecutive steps of chromatography purification.

We evaluated the effect of cholesteryl hemisuccinate (CHS) supplementation during the affinity purification steps of nAChR-LFC-16 in terms of receptor secondary structure, stability and functionality. CHS produced significant changes in the degree of  $\beta$ -secondary structure, these changes compromise the diffusion of the nAChR-LFC-16 in lipid cubic phase. The behavior was reversed by Methyl- $\beta$ -Cyclodextrin treatment. Also, CHS decreased acetylcholine evoked currents of *Xenopus laevis* oocyte injected with nAChR-LFC-16 in a concentration-dependent manner. Methyl- $\beta$ -Cyclodextrin treatment do not reverse functionality, however column delipidation produced a functional protein similar to nAChR-LFC-16 without CHS treatment.

### 1. Introduction

The nicotinic acetylcholine receptor (nAChR) has long been the Holy Grail of membrane protein structure research. The nAChR has been postulated fundamentally for the regulation of various physiological processes in the human nervous system [1]. Moreover, nAChR assists in the communication between extracellular and intracellular compartments of the cell [2]. Also, nAChR has been implicated in a web of neurological diseases including myasthenia gravis disease, schizophrenia, Tourette's syndrome, attention-deficit, hyperactivity disorder, autism, depression, anxiety, dementia, nicotine addiction, the neurodegenerative diseases Alzheimer's, and Parkinson's, as well as

HIV-associated dementia and inflammation [3–12]. The nAChR has shown to be an important pharmacological target for the development of new treatments for various neurodegenerative diseases. The nAChR is a typical example of a multimeric membrane complex that although it is one of the most widely studied ion channels, its X-ray structure has been difficult to achieve, [13,14]. A high-resolution structure of the nAChR and its complexes containing various nicotinic ligands is of crucial importance for the design of novel agents that target defined nervous system pathologies.

The nAChR was the first member of the Cys-loop and cation-selective pentameric ligand-gated ion channels (pLGICs) [13]. The bases of what we know today about the pLGICs is because of the structures obtained

\* Corresponding author. Department of the Biology, University of Puerto Rico, Río Piedras Campus, San Juan, Puerto Rico.  
E-mail address: [jlasalde@gmail.com](mailto:jlasalde@gmail.com) (J.A. Lasalde-Dominicci).

<https://doi.org/10.1016/j.ab.2020.113887>

Received 24 May 2020; Received in revised form 14 July 2020; Accepted 22 July 2020

Available online 4 August 2020

0003-2697/Published by Elsevier Inc.

from the acetylcholine-binding protein, which defined the structural bases of the extramembrane domains aiding the understanding of the interactions of agonists or antagonists in the binding site [15–17]. In 1982 the Heinrich Betz group isolated the Glycine receptor (GlyRs), however, the first X-ray crystallographic structure at 3.0 Å resolution of closed human GlyRs- $\alpha$ 3 homopentamer in complex with the selective antagonist strychnine was obtained in 2015 [18,19]. The same working group improved the resolution of the GlyRs to 2.6 Å in complex with a positive allosteric modulator [20]. The first purifications of Gamma-aminobutyric acid receptors (GABA<sub>A</sub>) isolated from bovine brain carried out by Eric A. Bernard using affinity chromatography [21]. The first crystal structure of a human GABA<sub>A</sub> was obtained at 3.0 Å resolution [22]. In 2014 the first X-ray structure of mammalian Serotonin receptors (5-HT<sub>3</sub>R) was obtained at a resolution of 3.5 Å in complex with nanobodies [23]. In addition, a new structure of 5-HT<sub>3</sub>R was recently obtained at 4.3 Å resolution using Cryo-EM technology [24]. Finally, different structures of the pLGICs of prokaryotic organisms have also been successfully attained, providing a better understanding of the structure of homologous channels [25–27].

In 1972 Jean Pierre Changeux and colleagues first isolated a nAChR protein sample from the electric tissue of the *Torpedo marmorata* [28]. During the past 3 decades, several research groups have unsuccessfully attempted to obtain a high-resolution structure of the nAChR. Toyoshima and Unwin initial attempts yielded a structure of the channel at 17 Å resolution determined by three-dimensional reconstruction from the image of tubular vesicles containing *Torpedo marmorata*'s nAChR [29]. Unwin and coworkers continued their efforts and improved the nAChR structure at 9 Å resolution using electron microscopic techniques, and finally a nAChR structure at 4 Å resolution [30–32]. More recently, a 2.7 Å resolution structure of  $\alpha$ -bungarotoxin bound to the nAChR was achieved by cryogenic electron microscopy (CEM). The nAChR was purified from *Tetronarce* or *Torpedo californica* electric tissue solubilized with Triton and later exchanged to *n*-Dodecyl  $\beta$ -D-maltoside (DDM) [33]. Moreover, in 2016 the same lab reported the first X-ray structure of the heteromeric neuronal  $\alpha_4\beta_2$  nAChR [34]. Although these structures have provided substantial information in nicotine binding, subunit stoichiometry, and overall oligomerization, these are low-resolution structures. Those obtained by CEM still present some structural issues, even the recently 2.7 Å resolution nAChR structure. Due to practical and modeling disadvantages, such as sample low signal to noise due to the low electron absorption of proteins, samples exhibit more beam-induced movement at tilt; the excess amount of ice cross section of a tilted frozen sample hinders image acquisition. Thus, only partial data has been used for structure reconstruction and refinement, which implies low quality and resolution. On this basis, higher resolution structural analysis is substantially needed for efficient ligand design for developing new pharmacological strategies for the neurodegenerative diseases that involve nAChR.

For decades, the solubilization, isolation and purification of nAChR from different sources have not been the most efficient, leaving different impurities in the purified nAChR in spite of the protocol used. Affinity purification, alkaline treatment, chaotropic salts and sucrose gradient are the methods regularly employed in nAChRs sample purification [35–38]. Impurities such as, ATPase, Rapsin, Calcium channels, Tyrosine kinase, Agrin receptor and low molecular weight proteins invariably were present at different degrees in all protocols assayed [39–47]. During the solubilization process detergents intercalate in the lipid membrane, breaking the existing intermolecular forces between lipid-lipid, lipid-protein and protein-protein, and then incorporate pieces of membranes in micellar structures that are surrounded by an aqueous environment. The size of the micelles and the ability of the detergent to protect the hydrophobic belt of the isolated protein depend largely on the physicochemical properties of the detergent. In this way, an ideal detergent should have the ability to mimic endogenous annular lipids and bear sufficient hydrophobic surface area, in order to decrease the hydrophobic mismatch of the protein. Integral membrane proteins

are buried in a hydrophobic environment of biological membrane and to achieve its isolation it is necessary to use detergents. Choosing a detergent correctly for solubilization purposes is a crucial step, if the isolated membrane protein is for structural and functional studies. This is particularly critical for membrane proteins which have lipid-dependent functionality such as the nAChR.

The lipid dependence of muscle nAChR and *Torpedo* has been postulated and studied for decades. The nAChR is an integral membrane protein composed of four homologous subunits with a stoichiometry with a  $2\alpha, \beta, \gamma$  and  $\delta$  arranged in a pentameric structure [48–51]. Each subunit traverses the membrane four times producing four trans-membrane regions (M1–M4), and all subunits are in contact with lipid molecules [32,52–55]. Given the hydrophobic profile of these subunits and both biochemical and molecular studies, different amino acid positions that are in contact with lipids have been postulated [56–61]. Due to its inherent topology and hydrophobic core embedded in lipid bilayer, the functional lipid dependence of nAChR is not surprising. The effect of phospholipids head group and its sn-2 substituted acyl hydrophobic fatty acids have been studied by the reconstitution of nAChR in model membranes [62–69]. Cholesterol is one of the most abundant lipids in biological membranes and its structure presents particular physicochemical characteristics that regulate the fluidity of the membranes [70]. The effects of cholesterol on nAChR stability and functionality have been studied by reconstitution of nAChR in model lipid bilayer at different mole fractions. The effect of cholesterol on the nAChR functionality has been extensively studied and reported [56,71–80].

In previous works we addressed the requirements of the nAChR solubilization from *Torpedo californica* without affecting functionality. Lipidomic studies were carried out for both, the whole electric organ tissue and nAChR detergent complexes with different lipid-like analogous detergents [39–42,81]. However, some impurities such as Rapsin remained in different degrees in all the purified nAChR with lipid-like detergents, being 1-palmitoyl-2-hydroxy-sn-glycero-3-phosphocholine (LFC-16) the most suitable detergent for the solubilization process [39,41,81].

In the present study we present an improved purification strategy for nAChR solubilized with LFC-16 detergent. The procedure involves the use of two steps of affinity chromatography, using pre-packed column with acetylcholine bromide coupled to Affi-Gel 15 and Capto Lentil Lectin (CLL) affinity chromatography prior to gel filtration chromatography (Fig. 1). The purity of the nAChR-LFC-16 was accessed using SDS-PAGE gels and Microfluidic Capillary Gel Electrophoresis (MCGE, Bio-analyzer). Our ultimate goal is to produce a pure and functional nAChR detergent complex for crystallization and X-ray diffraction purposes. For this we evaluated the nAChR-LFC-16 mobility on the lipidic cubic phase (LCP) by measuring the nAChR mobile fraction and diffusion coefficient through fluorescence recovery after photobleaching (FRAP) [39,81,82]. We also examined the functional characterization of nAChR-LFC-16 by recording macroscopic ion channel currents in *Xenopus* oocytes using the two-electrode voltage clamp [39,41]. Knowing the nAChR functional sensitivity to lipid environment, and taking into account the success obtained with the neuronal X-ray structure of the heteromeric, which was co-crystallized with cholesteryl hemisuccinate, we evaluated the effect of this cholesterol analog in terms of stability and functionality of the purified nAChR-LFC-16 complex using the sequential protocol.

## 2. Materials and methods

### 2.1. Materials

*Torpedo californica* electroplax tissue was obtained from Aquatic Research Consultants, (San Pedro CA). The cholesteryl hemisuccinate (CHS) (C6512), Methyl  $\alpha$ -D-mannopyranoside (67770), Carbamoylcholine Chloride (C4382), Bromoacetylcholine bromide (B121), Ultrafree-MC Centrifugal filters (UFC30GV25) and Amicon Ultra Centrifugal Filters 100 K, (UFC910096) were acquired from Sigma Aldrich (St. Louis,

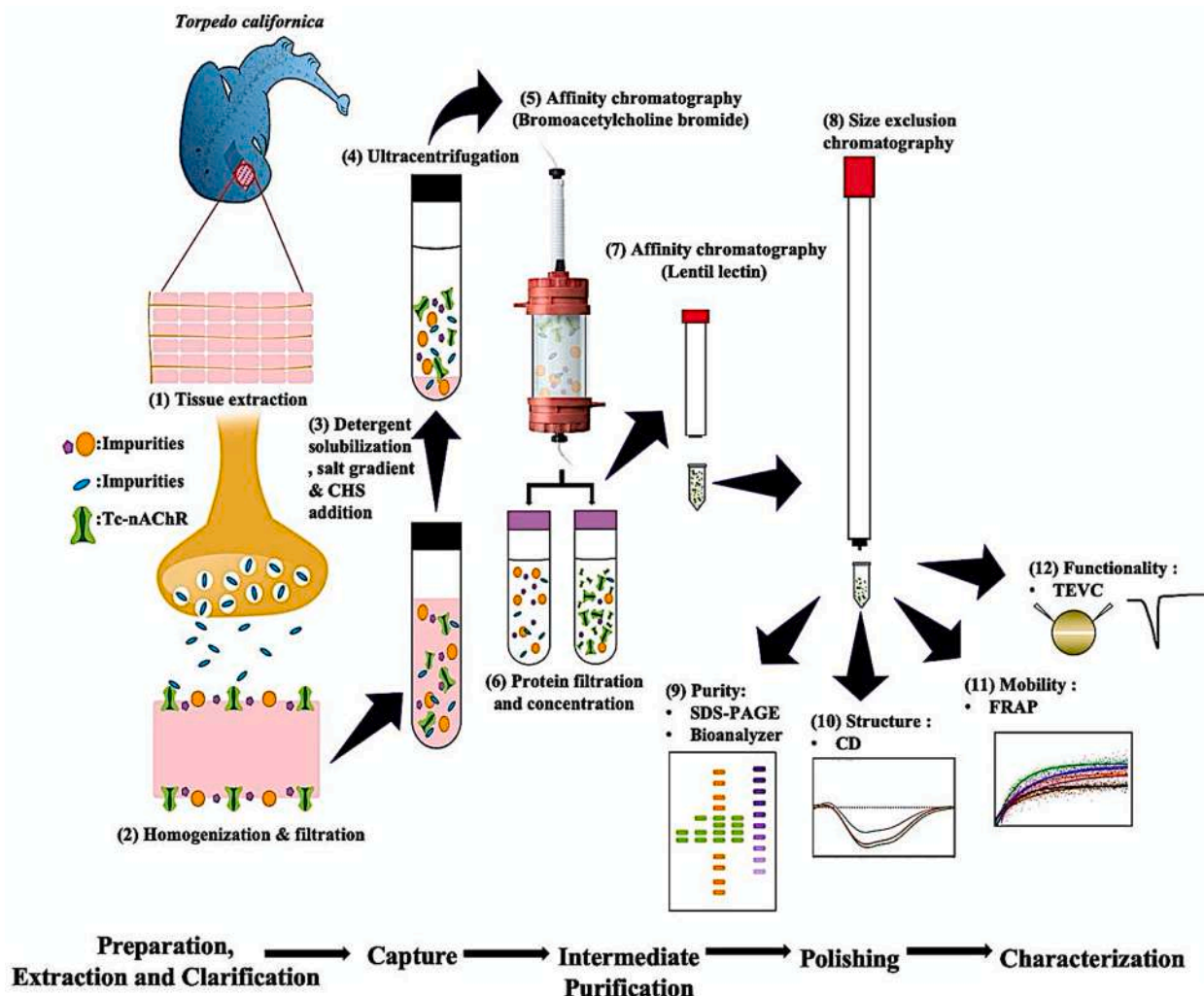


**Fig. 1. Improved purification and biophysical characterization of the *Torpedo californica*-nicotinic acetylcholine receptor in lipid-like detergent complexes (Tc-nAChR-DC).** The scheme presents the step by step the procedure used for the preparation of a highly pure, stable and functional nAChR-LFC-16 complex. The most relevant innovation involves a sequential purification system, which consists of (5 & 7) two steps of FPLC-affinity purification and (8) one step of FPLC-size exclusion chromatography. (9) Using SDS gels and Microfluidic Capillary Gel Electrophoresis (MCGE) Bioanalyzer, for the evaluation of protein purity. (10) We performed circular dichroism (CD) for the secondary structure predictions and (11) Fluorescence Recovery After Photobleaching (FRAP) using confocal microscopy for stability measurements in LCP. (12) Finally, we used the TEVC to access the functionality of the purified nAChR-LFC-16 injected into *Xenopus Laevis* oocyte.

MO). The 1-Palmitoyl-2-Hydroxy-sn-Glycero-3-Phosphocholine (LFC-16) (L216) were purchased from Anatrace (Maumee, OH). We have purchased the XK 16/20 empty column (28988937), HiTrap Capto Lentil Lectin (17548911) and Superdex 200 10/300 increase (28990944) from GE Healthcare Life Sciences (Marlborough, MA). Pierce detergent removal spin column (87777), Pierce bichoninic acid (23225) and  $\alpha$ -BTX, Alexa Fluor™ 488 conjugated (B13422) was purchased from Thermo Fisher (Waltham, MA). The High Sensitivity Protein 250 Assay Kit (5067-1575) has been purchased from Agilent (Santa Clara, CA). The Affi-Gel-15 (1536052) and 4–20% Criterion TGX Stain-Free Gel (5678093) was procured from Bio-Rad (Hercules, CA). All other chemicals used in this article were purchased from Sigma Aldrich (St. Louis, MO). The water used for all buffers or solutions preparations were purified through Milli-Q water purification system from Millipore (Burlington MA).

## 2.2. Enhanced purification and extraction of *Torpedo californica* nAChR

The native nAChR was solubilized from *Torpedo californica* electroplax tissue, according to the protocols described by Asmar-Rovira and Padilla-Morales [39,42] with the following modifications: The

membranes were solubilized in 3.5 mM LFC-16, 0.2 mM CHS, 300 mM NaCl and 40 mM Tris-HCl pH 7.4 for 1 h at 4 °C followed by ultracentrifugation at 162,600 g for 1 h at 4 °C. FPLC ÄKTA Explorer 100 (GE Healthcare Life Sciences 18111241) was used for all sequential chromatography steps. The first step of purification is affinity chromatography. We used affinity columns (XK GE columns) pre-packed with acetylcholine bromide coupled to Affi-Gel 15. The column was equilibrated with 2 column volumes of DB-1X (5  $\mu$ M LFC-16, 0.2 mM CHS, 10 mM MOPS, 0.1 mM EDTA and 0.02% NaN<sub>3</sub> (wt/vol), pH 7.4) at flow rate of 2 mL/min. Afterward, the solubilized membrane was injected into the first step of affinity chromatography at a flow rate of 1 mL/min. Then nAChR-DC was eluted with 13 mM carbamoylcholine chloride in DBS-1X buffer (5  $\mu$ M LFC-16, 0.2 mM CHS, 100 mM NaCl, 10 mM MOPS, 0.1 mM EDTA, 0.02% NaN<sub>3</sub>, pH 7.4) at flow rate: 2 mL/min. After elution from the column, microfiltration was performed with Ultrafree-MC centrifugal filter, for sample clarification. Subsequently, the second chromatography step was performed with HiTrap Capto Lentil Lectin affinity chromatography (CLL). First, the column was equilibrated with 10 column volumes of the equilibration buffer, consisting of 20 mM Tris-HCl, 500 mM NaCl and 0.5% sodium deoxycholate (wt/vol) pH 8.3 at a flow rate of 1 mL/min. Afterward, the nAChR-DC

was injected into the CLL at a flow rate of 0.5 mL/min. Subsequently, the nAChR-DC was eluted with 0.2 M methyl  $\alpha$ -D-mannopyranoside, 0.5% deoxycholate, 20 mM Tris-HCl and 500 mM NaCl pH 8.3 at flow rate of 1 mL/min. Collected sample fractions were concentrated using centrifuge filters with a 100 K cutoff. Then, size exclusion chromatography was performed as the last step of purification with a Superdex 200 10/300 increase Gel filtration GE column at a flow rate of 0.25 mL/min. The column was equilibrated with 2 column volumes of DB-1X pH 7.4. Lastly, the eluted protein was concentrated with Amicon 100 K cutoff. The protein concentration was determined by the method of the bicinchoninic acid assay (BCA). Finally, the purity was analyzed by microchip-based capillary gel electrophoresis (MCGE) and SDS-PAGE.

### 2.3. Purity analysis determination

The purity analysis determination of the purified nAChR-DC was performed with analyzed by microchip-based capillary gel electrophoresis MCGE with the Agilent 2100 bioanalyzer method, which provides highly precise analytical impurity detection of proteins using a stable covalent fluorescent dye to epsilon amino groups of lysine residues prior to automated protein purity detection on the MCGE for the nAChR-DC [83–86]. We used for the first time a high sensitivity protein purity assay (HSP-250 kit) for the nAChR-DC, which allows a sensitivity in picograms superior to traditional techniques such as silver-stained SDS-PAGE or coomassie-stained SDS-PAGE [84,85,87,88]. The MCGE assay was performed according to the protocols described in Agilent High Sensitivity Protein 250 Assay [85]. Briefly, 2.5  $\mu$ L of DB-1X buffer and 0.5  $\mu$ L of standard labeling buffer was mixed with 2  $\mu$ L of the purified sample to obtain a final protein concentration of 2  $\mu$ g. Subsequently, 0.5  $\mu$ L of dye was added to each sample tubes and incubated for 30 min on ice. Upon completion of the incubation period, 0.5  $\mu$ L of ethanalamine was used to stop the labeling reaction. Accordingly, the sample was diluted to a 1:100 ratio (sample: ultrapure water). Then 4  $\mu$ L of the labeled diluted protein was mixed with 2  $\mu$ L of 1 M dithiothreitol (DTT) using denaturant conditions at 95 °C for 5 min. Afterward, the denatured sample was cool down on the ice and spin down for 15 s. Finally, the HSP-250 gel matrix and samples were loaded on a microchip for purity analysis determination in the Agilent 2100 bioanalyzer assay [83–85].

### 2.4. On-column delipidation

The on-column delipidation of the purified nAChR-DC was performed with the pierce detergent removal spin column according to the method described by Antharavally with minimal modifications [89]. The spin column was centrifuged at 1500 g for 1 min to remove the storage buffer. The delipidation column was equilibrated with three volumes of 400  $\mu$ L of DB-1X buffer without CHS and centrifuged at 1500 g for 1 min. Then 100  $\mu$ L of the sample was injected into the column and incubated for 5 min at room temperature. Lastly, the sample was eluted by centrifugation for 2 min at 1500 g.

### 2.5. Functional characterization of nAChR-Detergent complex in *xenopus* oocytes

For the functional characterization of nAChR-DC prepared as described above, we used a protocol originally reported by Milely research group [90] which was modified and successfully performed by our group [39,40]. Defolliculated *Xenopus laevis* oocytes at stages V and VI were commercially obtained from Ecocyte (Ecocyte BioScience, Austin TX). Oocytes were incubated at 17 °C in ND-96 media containing in mM: 96 NaCl, 2 KCl, 1.8 CaCl<sub>2</sub>, 1 MgCl<sub>2</sub>, 5 HEPES, 2.5 Na-pyruvate; supplemented with gentamicin (50 mg/mL), tetracycline (50 mg/mL) and theophylline (0.5 mM); and adjusted to a pH of 7.6 with NaOH. Oocytes were microinjected with 50 nL of 3 mg/mL of nAChR-DC from *Tc* prepared supplemented with cholesterol (CHS), and CHS plus

Methyl- $\beta$ -Cyclodextrin treatment using a Nanoject II (Drummond Scientific, Broomall, PA).

### 2.6. Macroscopic ion channel functional assay

Macroscopic currents were measured using the Two-electrode voltage clamp (TEVC) technique 16–36 h after injection. Oocytes continuously perfused a calcium free OR-2 containing in mM: 82 NaCl, 2.5 KCl, 1 MgCl<sub>2</sub>, 5 HEPES; and adjusted to a pH of 7.6 with NaOH; and exposed to a 5 s application of 100  $\mu$ M acetylcholine was applied using a computer control 8 channel perfusion system (VC-8, Warner Instruments, Hamden, CT) at a holding potential of –70 mV using a Gene Clamp 500B amplifier (Axon Instruments, Foster City, CA). The electrodes were filled with a solution of 3 M KCl and the resistances were calculated to average 1.3 m $\Omega$ . Macroscopic currents were filtered at 100 Hz and digitized at 1000 Hz using a Digidata 1440A interface (Axon Instruments, Foster City, CA) and acquired using the Clampex 10.2, (pCLAMP 10.2 software, Molecular Devices) running on a Microsoft Windows-based computer.

### 2.7. Statistical analyses

Statistical analyses were performed using the GraphPad Prism 6 software (GraphPad Software, San Diego, CA, [www.graphpad.com](http://www.graphpad.com)). Data samples were analyzed separately using Two-way mixed model ANOVA and One-way ANOVA. All TEVC data were analyzed using a non-parametric unpaired *t*-test with a Mann Whitney post-analysis. Comparisons of the means for the individual treatments were made at the 5% significance level based on the F-test of the analysis of variance.

## 3. Results

### 3.1. Purification and purity analysis determination of the nAChR-Detergent complex

We have optimized the original protocol describing the purification of nAChR from its native *Torpedo californica* electric organ using lipid-like detergents. The intention behind this optimization is none other than to improve the purity level of the nAChR-DC without compromising its stability and functionality. The whole purification process of the nAChR-DC was improved by the implementation of several purification steps and sample preparation. We took into consideration the physicochemical characteristics of the receptor and used them as an advantage for the isolation of what until now was considered a burden in obtaining a clean preparation of nAChR-DC. This could be carried out thanks to the development of new commercially available efficient affinity columns. Fig. 1 presents the whole purification and characterization procedures for the nAChR-DC; briefly, the core chromatographic purification steps consist of three consecutive steps. The first step is affinity chromatography by acetylcholine bromide coupled to Affi-Gel 15 as an affinity column and nAChR-DC eluted with 19.24 mL of 13 mM Carbamylcholine Chloride, followed by a second affinity chromatography using Capto Lentil Lectin to eliminate non glycosylated proteins and a final size exclusion chromatography. All chromatographic steps used buffers supplemented with 0.2 mM cholesterol to maintain nAChR-DC stability. In our original reported protocol and other researcher's protocols the solubilization of nAChR-enriched crude membrane fractions was performed by sucrose gradient [42,81,91,92]. This step was eliminated and the solubilization was performed under a 3-fold increase of salt which represents a final concentration in the solubilization buffer of 300 mM NaCl. In addition, the final concentration of the detergent employed in the solubilizing step was 3.5 mM and decreased substantially to 1.5 times the critical micelle concentration (CMC) for the subsequent chromatography steps. Another important change to our original protocol was the use of Affi-Gel 15 instead of Affi-Gel 10 due to a better interaction of the former with proteins that exhibit slightly acid

isoelectric point. The comparison of the purified nAChR-DC protein profiles using our original and the improved protocol is presented in Fig. 2; the absorbance at 280 nm of each eluted protein peaks were monitored at different elution volumes. The peripheral protein impurities that invariably accompany nAChR-DC purification in any reported purification protocol have been removed in our improved protocol (Fig. 2 a and b). The molecular weight range of the nAChR-DC subunits and impurities also has been assayed by SDS-PAGE electrophoresis. Fig. 2 (c, d and e) presents the characteristic  $\alpha\beta\gamma\delta$  bands for the purified nAChR-DC in the traditional and improved protocols. The nAChR-DC purity was improving since the first chromatographic step as compared to our original protocol, with 46% of purity, 88% purity after Capto Lentil Lectin column, and average nAChR-DC purity of 94% nAChR-DC for the gel filtration step.

### 3.2. Macroscopic ion channel functional assay

Consistent with what we previously observed in Báez et al., 2016, the TEVC results suggest that increasing cholesterol concentration in the LFC-16-nAChR-DC significantly reduces the ACh-induced macroscopic peak currents in *Xenopus laevis* oocytes [78]. When not supplemented with CHS (control), mean peak amplitudes average  $-363 \pm 29$  nA ( $n = 5$ ) (Fig. 3a). However, as CHS concentration increases, the peak amplitude of the responses are significantly reduced; at 0.1 mM CHS the amplitude is  $-184 \pm 41$  nA ( $n = 5$ ;  $p = 0.008$  when compared to control) (Fig. 3b) and at 0.2 mM CHS the amplitude is  $-50 \pm 4$  nA ( $n = 7$ ;  $p = 0.003$  respectively when compared to control) (Fig. 3c). To evaluate the reversibility of cholesterol supplementation, nAChR-LFC-16 was treated with Methyl- $\beta$ -Cyclodextrin. The Methyl- $\beta$ -Cyclodextrin treatment was

able to substantially improve the nAChR-LFC-16 mobility in LCP experiments presented in the data in brief, however it was not able to reverse functionality in TEVC (Fig. 3d). Oocytes treated with Methyl- $\beta$ -Cyclodextrin evoke currents with amplitudes of  $-46 \pm 6$  nA ( $n = 11$ ; compared to  $-50 -50 \pm 4$  nA for 0.2 mM CHS) (Fig. 3d). Interestingly, when the same sample was partially delipidated using Pierce Detergent Removal Spin Column, the result was reverted levels ( $-320$  nA  $\pm 35$  nA,  $n = 4$ ; compared to  $-363 \pm 29$  nA in control) (Fig. 3e). It is imperative to mention that the most recently nAChR structure obtained by CryoEM used DDM as the final exchange detergent. The activity of nAChR-DDM complex measured by TEVC resulted in mean ACh evoked responses ( $-12 \pm 2$  nA), 0.45% of that evoked by the nAChR-LFC-16 [39]. These results cast doubt on the ability of DDM to preserve receptor functionality, although results reported by Rahman 2020, of the nAChR-DDM activity measured by liposome patch-clamp electrophysiology experiments at a holding potential of  $\pm 50$  mV and  $-75$  mV exhibited opening amplitude of near 6 pA inherent to this technique [33].

### 4. Discussion

Despite all the efforts made by different groups to obtain a functional crystallographic structure of the nAChR, a successful high-resolution X-ray structure has not been obtained so far. All of these efforts have been unsuccessful due to various pitfalls throughout all stages of the nAChR purification process including its solubilization. We have handled problems related to the solubilization process through the use of lipid-like detergents which minimize the loss of essential annular lipids to maintain the activity of nAChR in the detergent complex [39,41,81]. However, the greatest barrier that has arisen in the purification of

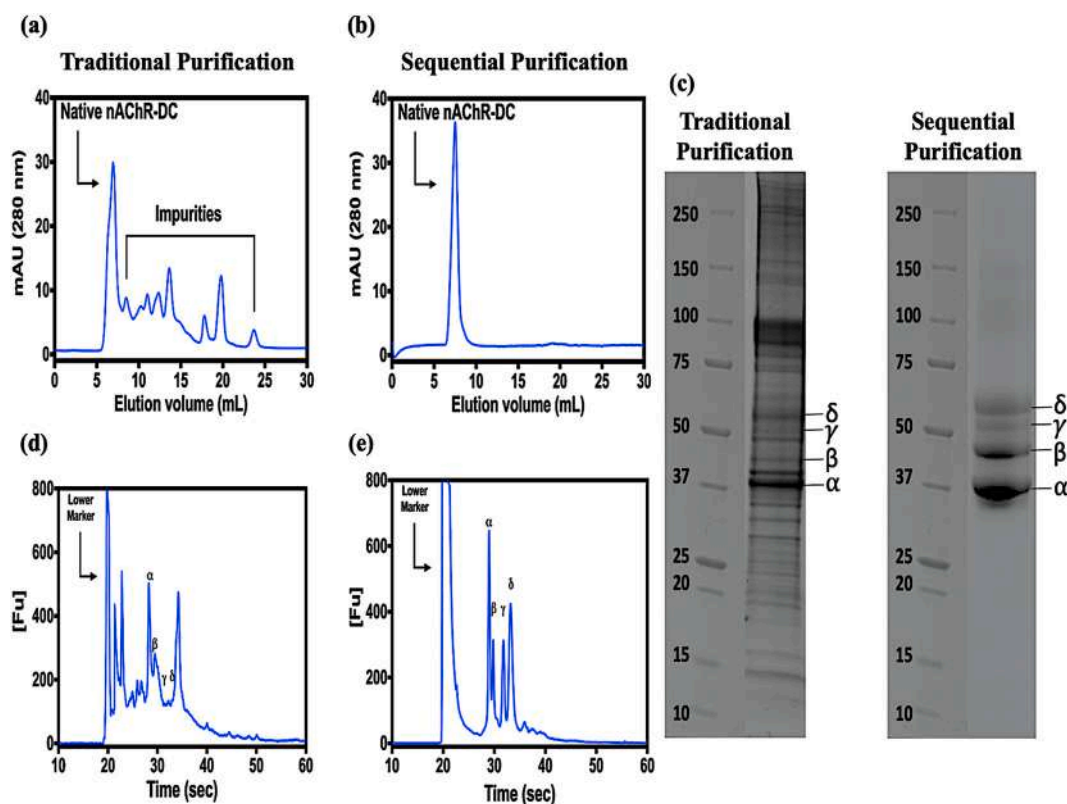


**Fig. 2.** Comparison of the traditional and improved sequential purification of *Torpedo californica* nAChR-LFC16 complex. Chromatography was performed using a Superdex 200 10/300 increase Gel filtration GE column, flow rate of 0.25 ml/min. The elution profile was monitored at 280 nm. (a) Elution profile *Tc*-nAChR-LFC-16 using traditional chromatographic procedure. (b) Elution profile of the same preparation, but using sequential FPLC-Affi-Gel 15-Capto Lentil Lectin-SEC purification steps, (c) SDS-PAGE 4–20%, protein migration patterns for both purification protocols (left) traditional chromatography, (right) sequential purification, and (d and e) Microfluidic Capillary Gel Electrophoresis electropherograms showing the nAChR characteristic  $2\alpha\beta\gamma\delta$  bands for the traditional and sequential protocols.

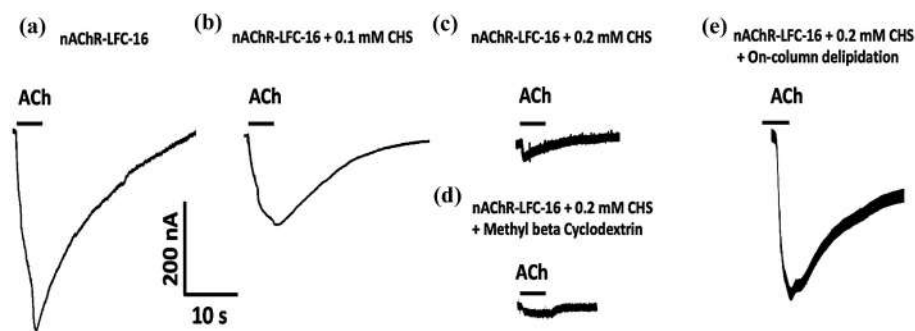


**Fig. 3.** Macroscopic ion channel functional responses of LFC-16 solubilized and purified nAChR-DCs supplemented with different concentrations of cholesterol. Protein samples corresponding to purification under different conditions were micro-injected into *Xenopus laevis* Oocytes; and responses were induced by a 5 s application of 100  $\mu$ M ACh, measured (represented by bars) at  $-70$  mV. Conditions tested were (a) without cholesterol (No CHS,  $n = 5$ ) with different concentrations of CHS ((b) 0.1 mM,  $n = 5$ ; & (c) 0.2 mM,  $n = 7$ ), (d) with supplementation of Methyl- $\beta$ -Cyclodextrin ( $n = 11$ ) and (e) following delipidation ( $n = 4$ ).

nAChR has been the protein impurities that co-elute with nAChR due to their association in the native membrane. In this work we optimized our previous purification process using three sequential chromatographic purification steps consisting of one affinity chromatography with acetylcholine bromide coupled to Affi-Gel 15 and followed by a second affinity chromatography using CLL to eliminate non-glycosylated proteins, and a final gel filtration. Furthermore, the resulting nAChR-LFC-16 complex under the purification conditions used were tested in terms of mobility in LCP, and functionality. In addition, nAChR-LFC-16 crystals were harvested using a new device developed in our laboratory the RMP@LMx (U.S. patent 10,155,221, provisional patents 15996946 and 15997728 for devices proposed). Examples of crystal harvest performed and diffracted at Argonne Advance Photon Source facilities are in the data in brief [93].

In our previous purification procedure, we used Affi-gel 10 coupled to acetylcholine bromide as an affinity chromatography, while in the improved procedure an Affi-Gel 15 was used. Affi-Gel is nothing other than agarose modified with N-hydroxysuccinimide esters. The rationale behind this change lies in the isoelectric pH of the nAChR which is estimated to have a value of 5.6. Binding studies of different proteins to Affi-Gel 10 and 15 demonstrated that proteins at pH near or below its isoelectric point couples best to Affi-Gel 10, and that Affi-Gel 15 is more efficient binding proteins at pH near or above its isoelectric point [94]. The change to Affi-Gel 15 helps not only to increase the purity of the nAChR-LFC-16 complex by removing muscle skeletal receptor tyrosine-protein kinase, ATPase and high molecular weight proteins greater than 200 kDa (Fig. 2 c left), but to improve the overall protein yield. The purification of native muscle-type nAChR from *Torpedo californica* that led to the 2.7 Å resolution by CEM, used a single affinity purification followed by size exclusion chromatography and produced a dimeric receptor. These results are not surprising since, DDM induced the formation of 25% and 50% of aggregates and monomers for the nAChR, respectively [42]. The authors tried to increase the ratio of monomer: dimer by 50 mM  $\beta$ -mercaptoethanol reduction treatment [33]. The innovation of this purification was the use of NHS-activated Sepharose 4 Fast Flow coupled to an agarose matrix (2 - [(4-aminobutanoyl) amino] -N, N, N-trimethylethanamine) for the affinity chromatography. However, the purity of the eluted protein as shown on the SDS PAGE still have Rapsyn traces and Na<sup>+</sup>/K<sup>+</sup> dependent ATPase, and other traditional impurities cannot be observed because the bands beyond 75 MW are not showed on the gel [33]. These high molecular weight contaminants were observed after 100 mM  $\beta$ -mercaptoethanol reduction treatment of the purified nAChR from *Torpedo californica* [95].

The first purification protocols for the nAChR from the electrical organ of *Electrophorus electricus* and *Torpedo marmorata* were carried out using columns packed with solid supports conjugated with different toxins extracted from cobra venoms. Although this strategy produced good performance, the functionality and purity of the isolated protein were compromised. In these cases, between 120 and 1000 g of the initial tissue were used and the amount of nAChR obtained was in a range of

2.3 and 50 mg respectively [92,96]. Our Affi-Gel 15 coupled to acetylcholine bromide produced approximately 4 mg of highly pure nAChR-LFC-16 from a starting 40 g of *Torpedo californica* electric organ. This implies an increase in the yield of nAChR-LFC-16 of approximately 3-fold.

The lipid requirements of the nAChR and its homologues receptors in order to conserve stability and to undergo agonist-induced state transitions have been highly documented [64,71,97–103]. The nAChR lipid requirement is not only limited to the type of phospholipid head-group, but its esterified fatty acid. Also, the number of cholesterol molecules in the inner annular lipid shell surrounding the receptor transmembrane core are important [54,73,100,103,104]. The X-ray structure of the human  $\alpha 4\beta 2$  nicotinic receptor at 3.9 Å was achieved by diffracting crystals that were obtained by co-crystallization with the agonist nicotine and CHS [34]. Taking into account the lipid requirements of nAChR from *Torpedo californica* and the success attained using CHS for the  $\alpha 4\beta 2$  nicotinic receptor structure, we decided to supplement all the buffers for the purification steps. CHS was initially used as a cholesterol substitute for the modulation cell membrane fluidity. Since cholesterol molecules were observed in protein complexes diffracted by X-rays, it has been attempted to use cholesterol-like molecules for the process of solubilization of membrane proteins [34,105–107]. One of these molecules has been CHS however; its structure is slightly different from that of cholesterol. CHS contains an ester group, which gives it a negative charge at neutral pH, making it more hydrophilic than cholesterol.

The determination of the best CHS concentration for nAChR-LFC-16 purification using different CHS concentrations, ranging from 0.01, 0.1, 0.2 and 0.5 mM to supplement the solubilization and subsequent chromatography steps without CLL is presented in the data in brief [93]. The results consistently demonstrated that 0.2 mM CHS, disassembly of receptor subunits is minimized and a cleaner signal of the native nAChR-LFC-16 was obtained. This behavior was also confirmed by SEC and SDS-PAGE of the flow through, wash and elution of affinity chromatographic step [93]. The others CHS concentrations presents high values, they contain contaminants or affect the receptor stability by beginning to disassemble the subunits. Although CHS buffers supplementation in the affinity purification steps substantially removes impurities that were traditionally observed by SDS-PAGE from the nAChR-detergent complex, care must be taken to preserve stability, particularly in regards to the effect those CHS molecules excessively incorporated on the surface of the lipid/detergent belt that cover the hydrophobic region of nAChR, could have in the nucleation process in the LCP. During the nucleation and crystal growth processes in LCP, the membrane proteins must have an adequate average mobile fraction over a period of several weeks [108–111]. The possibility of nAChR-LFC-16 aggregates or oligomers due to CHS treatment could restrict the translational diffusion because of the physicochemical properties of hydrated monoolein at the cubic-Pn3m mesophase. Due to this, diffusion is highly dependent on the native three-dimensional conformation of nAChR-LFC-16. In order to evaluate this constraint, CD spectrometry assays were carried out for each treatment used during the purification

of nAChR-LFC-16 complex prior to diffusion experiments. For more details of the CD results see our data in brief [93].

CHS supplementation induces a significant change in favor of  $\beta$  structures and total loss of  $\beta$  turns and slightly increases the thermal denaturation temperature compared to the nAChR-LFC-16 without CHS treatment. This behavior is not unique to the nAChR-DC preparation since, membrane proteins and soluble proteins exhibit amino acid sequences that provide consensus cholesterol-binding motifs, known as Cholesterol Recognition Amino acid Consensus (CRAC), or inverted CARC, when amino acid consensus sequence exhibits the opposite orientation along the polypeptide chain [112–114]. Despite the increase in the number of X-Ray determined membrane protein structures, which showed resolved lipids such as cholesterol, there are not enough studies to correlate function with the presence of these lipids [115–119]. Furthermore, an overview of 73 crystallographic structures with cholesterol-bound of soluble and membrane proteins have shed light into the structural characteristics of cholesterol binding, where in the majority of the cases studied, cholesterol is positioned with its  $\alpha$ -face oriented toward the  $\beta$ -strands and its  $\beta$ -face facing the  $\alpha$ -helical structure [120]. CARC motifs have been identified in the *Torpedo californica* nAChR [77,105,121,122]. Experimental evidence supports the hypothesis that cholesterol induces amyloid-beta aggregation by increasing  $\beta$ -sheet formation and aromatic side chain mutation eliminate the cholesterol aggregation effect [123,124]. This  $\beta$ -sheet formation effect could be explained in terms of  $\pi$ - $\pi$  stacking of cholesterol steroid group and the benzyl group of phenylalanine and/or tyrosine. Moreover, cholesterol and its analogs have other regions that could stabilize the native secondary structures of the protein or induce transitions to other secondary structures. These regions are found in the 3 $\beta$ -Hydroxy-5 cholestene and CHS molecules in the carbons (C7, C12, C21, and C26). In CHS the hydroxyl at position C3 is replaced by the 3-hemisuccinate group which does not affect the interactions in the aforementioned carbons. However, the 3-hemisuccinate group is C3-esterified and at the hemisuccinate tail end contains a carboxylic group, which has a higher negative charge density at physiological pH than cholesterol hydroxyl group. The  $\text{C}=\text{O}$  portion of this head group function as a hydrogen-bond acceptor and the deprotonated carboxylic acid will form in addition to hydrogen-bond, electrostatic interaction with charged amino acids.

The physicochemical properties of detergents and lipids in the vicinity of proteins can modulate the degree of its secondary structures and, in turn, the thermal stability of the protein and its functionality [118,125–127]. In other hand, some  $\alpha$ -helices situated between  $\alpha$ -helix could be protected by its hydrophobic environment from alpha to beta transitions. However, a change in the physicochemical properties of the surroundings, such as the one provided by CHS in the nAChR-LFC-16 DC can change the tendency and favor the alpha to beta strand transition [128,129]. The presence of 0.2 mM of CHS in the nAChR-LFC-16 complex produces an increase in the content of  $\alpha$ -helix,  $\beta$ -strand anti-parallel and parallel of 3.1%, 5.5% and 16.6% respectively (See Table 1 in Ref. [93]). This suggests that CHS is promoting the  $\alpha$ -helix or other secondary structure to  $\beta$ -strand transitions through hydrophobic interactions, hydrogen and salt bridges with amino acids in the locality where it is found. The numbers of turns were diminished and the other types of structures are also drastically decreased by 14.3%. Methyl- $\beta$ -cyclodextrin treatment of nAChR-DC was used with the intention of eliminating excess CHS, although we understand that it can also eliminate other endogenous lipids that co-solubilized with nAChR. This treatment has a significant effect on  $\alpha$ -helix and parallel  $\beta$ -strand content and increased more than 2-fold the percent of  $\beta$ -strand anti-parallel compared to the nAChR-LFC-16 alone. Also, the percent of turns and other possible secondary structure were restored to similar nAChR-LFC-16 complex values. A decrease in  $\alpha$ -helices produces a decrease in melting temperature measured at 222 nm. Changes in the content of secondary structures are in agreement with the thermal stability of the preparations [118,130].

Evidently, CHS supplementation apparently produces some degree of perturbations of the lipid environments of the nAChR-LFC-16 that can traduce to a protein structure altering the diffusion rate in LCP. A complete explanation of the FRAP results is explained upon at data in brief [93]. The diffusion properties within the LCP matrix were found to be highly dependent on the stability of the protein detergent complex [39,81,108]. The mobile fraction drastically decreases throughout the 30-day period studied for all sample supplemented with CHS (See figure in Ref. [93]). Apparently, CHS supplementation produces some degree of molecules intercalation in the lipid annular lipids of the nAChR-LFC-16 producing conformational changes in the protein structure, which alter the diffusion rate in LCP. The diffusion properties within the LCP matrix have been found to be highly dependent on the stability of the protein [108]. Our previous FRAP studies in which cholesterol analogue detergents 3-[(3-cholamidopropyl) dimethylammonio]-2-hydroxy-1-propanesulfonate (CHAPSO) and sodium cholate 3 $\alpha$ ,7 $\alpha$ ,12 $\alpha$ -Trihydroxy-5 $\beta$ -cholan-24-oic acid (Cholate), were used as the primary membrane solubilizing agent showed no considerable diffusion differences during the 30-day period and a  $\Delta$ FFR value of 0.5 and 0.09 respectively [39]. It is clear that CHS differs structurally from the aforementioned cholesterol analogs and CHS is produced from a modification in the OH of the cholesterol head group, and the contrary CHAPSO and Cholate are derived from modifications in the alkyl side chain of cholesterol molecules. However, CHS in our protocol is not the primary solubilizing agent, but its presence seems to produce similar effects diffusion coefficient magnitude showing an average in the range of 10–9 cm<sup>2</sup>/sec during the 30-day period assayed. This represents a difference in the order of one magnitude less compared to the nAChR-LFC-16 [39,81].

To our best knowledge, this is the first time that a nAChR-detergent complex isolated and purified from *Torpedo*-rich membranes has undergone secondary structure assay without being reconstituted in a lipid mixture. Previous works have shown the secondary structure predictions of the entire or individual subunits of the nAChR purified by traditional methods or attained by recombinant technologies and reconstituted in different phospholipid, phospholipid/cholesterol, [98,131–136]. The invariable take home message in all reported studies was that the degree and composition of secondary structures is highly dependent on the lipid environment where nAChR is buried as a complete protein, or for its individual subunits. This behavior has not been the exception in our CD results, since the presence of CHS in the native lipid environment of nAChR-LFC-16 produced different degrees of alterations in the secondary structure of the receptor. The destabilizing effect of CHS is not only on stability, but it significantly affects the amplitude of the current measured in *Xenopus* oocytes injected with the nAChR-LFC-16 obtained from the purification supplemented with CHS (Figs. 3 and 4).

Early activity assay performed in planar lipid bilayer characterization using our previous purification procedure with zwitterionic cholesterol-analog detergents CHAPSO a sulfobetaine derivative of cholic acid and Cholate retained ion channel function. Both present comparable ion channel traces; mean ion channel current values for CHAPSO and Cholate were  $-1.92 \pm 0.04$  pA and  $2.48 \pm 0.03$  respectively [42,81]. However, CHAPSO and Cholate nAChR detergent complexes present more aggregates and monomers than monomers at the gel filtration profile [42,81]. Also, macroscopic currents were obtained using TEVC for nAChR-Cholate or nAChR-LFC-16. Results demonstrated that after 5 s application of 100  $\mu$ M acetylcholine (ACh) to an oocyte injected with nAChR-Cholate or nAChR-LFC-16 resulted in normalized amplitude with respect to the crude membranes of 1.0 and 1.32 respectively. These responses were completely abolished by the addition of  $\alpha$ -BTX [39]. We carried out TEVC for the nAChR-LFC-16 purified with buffer supplements with different CHS concentrations (Figs. 3 and 4). The results showed a significant reduction in ACh evoked macroscopic peak current which appears to be CHS concentration dependent (Fig. 3 a, b, and c).

This suggests that CHS not only affects the fluidity of nAChR-LFC-16

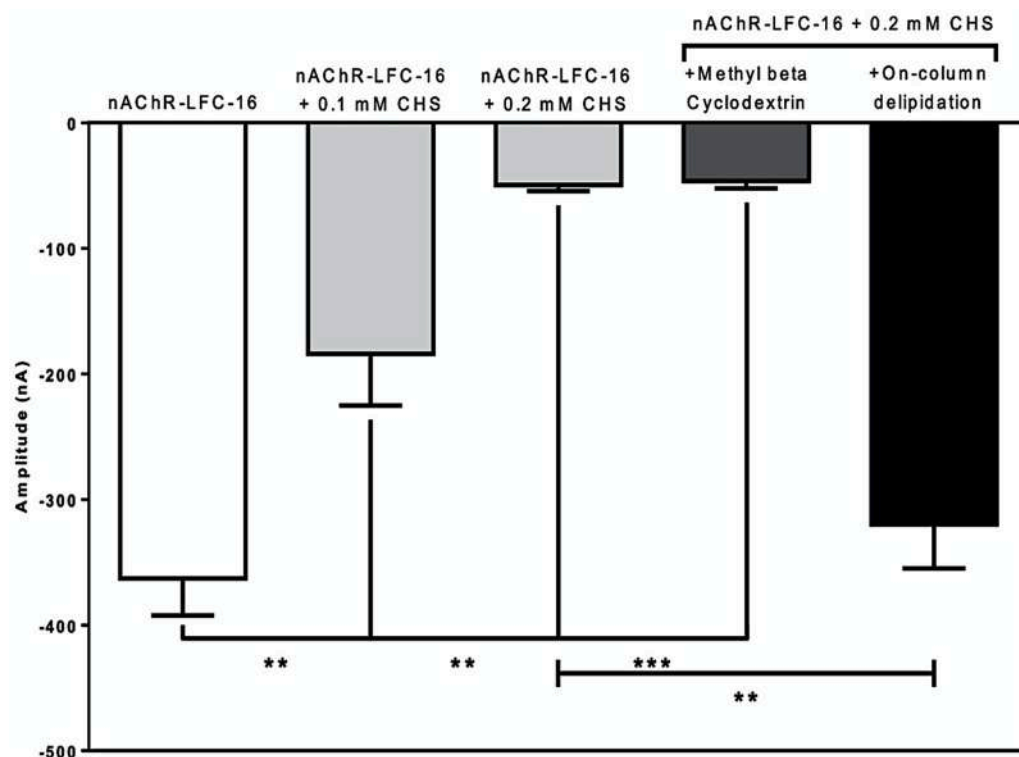


**Fig. 4.** Mean current amplitudes of LFC-16 solubilized and purified nAChR-DCs supplemented with different concentrations of cholesterol. Conditions tested includes: (a) nAChR-LFC-16 DCs without cholesterol (white bar); nAChR-LFC-16 DCs supplemented with either 0.1 mM and 0.2 mM cholesterol (light gray bars); with nAChR-LFC-16 DCs supplemented with 0.2 mM cholesterol and Methyl- $\beta$ -Cyclodextrin (dark gray bar); and nAChR-LFC-16 DCs supplemented with 0.2 mM cholesterol run through a delipidation column (black bar). Mean amplitudes were analyzed and compared using an unpaired non-parametric *t*-test with a Mann Whitney analysis (\*\**p*  $\leq$  0.01, \*\*\**p*  $\leq$  0.001).

in LCP, but also that it somehow alters the conformation of nAChR-LFC-16 in the *Xenopus* oocyte membrane. This behavior could be attributed to the changes in the degree of the secondary structure produced by the presence of CHS in nAChR-LFC-16. Furthermore, CHS can mimic cholesterol much more accurately than other analogous cholesterol detergents that we have previously studied, since the hemisuccinate is substituted in the same spatial region as the usual head group of cholesterol. In this way it can diffuse into the annular lipids surrounding nAChR-LFC-16 and carry out direct molecular interactions with amino acids at specific subunit special positions. Using the Unwin nAChR structure at 4 Å resolution and molecular dynamics simulations, three distinct cholesterol binding sites per subunit have been revealed [100]. Also, similar simulation and docking in  $\alpha 4\beta 2$  nAChR showed that anionic lipids and cholesterol could potentially modulate the channel gating transition via direct interactions with specific amino acids in the receptor subunits [137]. Taking into consideration that CHS mimic cholesterol physicochemical properties, it could be causing two types of effects: one directly interacting with the subunits and altering the functionality of the nAChR-LFC-16, and the second effect could occur when CHS interact with the lipid region that surrounds the receptor. In the latter, the functionality of the nAChR-LFC-16 could be affected by changes in fluidity that prevents the necessary conformational changes for gating [56,71–73,99,138–140]. To evaluate these possibilities, we used Methyl- $\beta$ -Cyclodextrin in order to remove excess CHS molecules from the nAChR-LFC-16 prior to be injected into oocytes for TEVC studies. Methyl- $\beta$ -Cyclodextrin treatment at 0.5 mM/1 h was unable to reverse the functionality of the nAChR-LFC-16 purified under CHS supplementation (Fig. 3 d). This result suggests the possibility of CHS interacting directly with the nAChR subunits, since the Methyl- $\beta$ -Cyclodextrin treatment used was strong enough to remove CHS from the peripheral boundary lipids in the nAChR detergent complex. Moreover, the change in degree of secondary structure measured by CD suggests a direct effect in which the CHS could be in contact with the nAChR subunits. Furthermore, Methyl- $\beta$ -Cyclodextrin treatment reversed the reestablishment of nAChR-LFC-16 mobility and diffusion through LCP [93]. Is important to highlight that the human  $\alpha 4\beta 2$

nicotinic receptor X-ray structure was successfully achieved by co-crystallization with CHS using vapor diffusion technique and the stability and activity of the  $\alpha 4\beta 2$ -DC were never determined prior to crystallization.

Methyl- $\beta$ -Cyclodextrin has been the most widely used method for acute cholesterol depletion to increase the fluidity of membranes, however this treatment appears to be not strong enough to remove cholesterol molecules that are embedded in membrane proteins cavities. To address this possibility, we carried out partial delipidation of the nAChR-LFC-16 supplemented with CHS using Pierce Detergent Removal Spin Column. Delipidated nAChR-LFC-16 injected into *Xenopus* oocyte results in average ACh evoked responses of  $-320 \text{ nA} \pm 35 \text{ nA}$ , which is similar to the nAChR-LFC-16 without CHS supplementation (Fig. 3 e and a). Seemingly, CHS supplementation induces highly specific interaction of CHS molecules with nAChR subunits which results in distortion in the extracellular portion of the receptor. Apparently the delipidation column was unable to remove all of the CHS molecules, leaving a pool of nAChRs whose tertiary structure reflects distortion by direct interaction with CHS. The cholesterol effect in the dynamics and the organization assembly of lipid bilayer fluidity has been reported previously as an allosteric effector on ligand binding sites in nAChR [56,61,98,99, 140–142].

In our previous report we found that detergent used to complex and extract *Tc*-nAChRs are able to alter the functionality of the receptor [39]. On that report we found that LFC-16 is a detergent that has the least alterations in functionality associated with their *Tc*-nAChRs DCs, when the native *Tc*-nAChRs crude membranes were homogenized and injected in oocytes, we found a desensitization half-time ( $dt_{1/2}$ ) of  $5.59 \pm 1.65 \text{ s}$  [39]. On that same study solubilization with LFC-16 forming *Tc*-nAChRs-LFC-16-DCs resulted in a  $dt_{1/2}$  of  $6.11 \pm 0.29 \text{ s}$ . In this study we are seen slowed desensitization kinetics in comparison to that previous study  $11.87 \pm 0.78 \text{ s}$ , this could be a result of the changes that we have done to the purification protocol which were necessary to achieve a higher purity of nAChRs. However, when comparing the desensitization kinetics among the different treatments shown we have found that as expected, as the cholesterol concentration increases the changes in

desensitization kinetics of the resulting Tc-nAChRs-DCs become more significant ( $dt_{1/2}$  0.1 mM CHS  $8.04 \pm 1.36$  s,  $*p = 0.0317$ ;  $dt_{1/2}$  0.2 mM CHS  $2.48 \pm 0.57$  s,  $**p = 0.0079$ ), which is consistent with what the behavior observed on Tc-nAChRs following cholesterol enrichment [78]. Interestingly addition of Methyl- $\beta$ -cyclodextrin to 0.2 mM CHS partially reversed some of the effect on desensitization kinetics  $3.95 \pm 2.05$  s (nAChR-LFC-16  $11.87 \pm 0.78$  s; 0.2 mM CHS  $2.48 \pm 0.57$  s). Furthermore, on-column delipidation of nAChR-LFC-16 samples enriched with 0.2 mM CHS completely reversed the desensitization kinetics of the channel ( $9.20 \pm 1.02$  s vs  $11.87 \pm 0.78$  s nAChR-LFC-16,  $p = 0.1111$ ), suggesting that removal of the enriched lipids is able to reverse the functional deficiencies associated with the addition of cholesterol used in the purification procedure.

The main objective of this study was to evaluate the effect of CHS supplementation during nAChR purification from the *Torpedo californica* electric organ using our improved purification protocol and also to examine the nAChR-LFC-16 functionality for future crystallographic attempts. Our improved purification strategy has successfully produced nAChR detergent complex with a higher degree of purity that makes it available for more robust studies including high throughput crystallization trials (Fig. 2). In this study we evaluated the use of CHS as a supplementary lipid to ameliorate the loss of essential lipids during the solubilization process of membrane proteins. Our focus of interest for several years has been the purification of the nAChR from *Torpedo californica* electric tissue in order to obtain a functional X-ray structure. The results presented here suggest that greater caution should be exercised in seeking to supplement the lipid needs of lipid-dependent transmembrane receptors, if a functional structure is to be obtained.

## 5. Conclusion

For a long time, hard work has been done to obtain a crystallographic structure of the nicotinic acetylcholine receptor in *Torpedo californica* at high resolution by implementing lipid-analogous or non-analog detergents [39,40,42,81]. Obtaining this nAChR atomic structure at high resolution by crystallography has had several obstacles such as purity and stability of protein in detergent complexes, making it difficult to obtain a crystal for X-ray diffraction. For that reason, our main objective was to improve and characterize the preparation of nAChR-DC in *Torpedo californica* in its natural state supplemented with CHS. We achieved what decades of independent laboratories effort and work had not been able to accomplish using new solubilization processes, which integrate small adjustments of CHS, NaCl and LFC-16 to improve extraction and purification process. Additionally, we optimized our previous purification process using three sequential chromatographic purification steps consisting of one affinity chromatography with acetylcholine bromide coupled to Affi-Gel 15, followed by second affinity chromatography using CLL to eliminate non-glycosylated proteins and final gel filtration. Finally, we have demonstrated the CHS effect in terms of mobility in LCP, secondary structure and function of the nAChR-DC under the purification conditions. With this work, we have been able to significantly improve and optimize the production of native nAChR-DC in its purest form without affecting the functionality and stability of the protein detergent complex.

## Author contributions

Rafael Maldonado-Hernández, Orestes Quesada, and José A. Lasalde-Dominicci: designed the experiments and optimized the protocol. Rafael Maldonado-Hernández, Orestes Quesada, and José O. Colón-Sáez: performed the experiments and contributed to the data analysis. Rafael Maldonado-Hernández, Orestes Quesada: initial draft and Orestes Quesada, and José A. Lasalde-Dominicci: edited and completed the finalized version of the manuscript.

## Declaration of competing interest

The authors declare no competing financial interests.

## Acknowledgments

This research was supported by; The National Institutes of Health NIGMS Grant: 1R01GM098343 (JALD, OQ) and supported by the National Institute of General Medical Sciences (NIGMS) of the National Institutes of Health (NIH) under Award Number P20GM103642, (JALD), COBRE NIEF Grant: 1P20GM103642 (JALD), Infrastructure support was provided in part by the National Institute on Minority Health and Health Disparities RCMI Grant: 2U54MD007600 (JALD), UPR-RP RISE Program Grant: 5R25GM061151(OQ, RMH) and BioXFEL STC of the National Science Foundation (NSF) Grant: 1231306 (RMH).The X-ray data was collected on the beamline 23-ID-B at Advanced Photon Source supported by U.S. Department of Energy, Office of Science, Argonne National Laboratory under Proposal ID 68121.The authors would like to thank the following students for their help: Edgardo Albino. Claude A. Maysonet-Navarro, Adriana Pastrana-González, Gloriangely Avilés-Reymundí and Manuel J. La Torre Poueymirou.

## References

- [1] M. Zoli, F. Pistillo, C. Gotti, Diversity of native nicotinic receptor subtypes in mammalian brain, *Neuropharmacology* 96 (2015) 302–311, <https://doi.org/10.1016/j.neuropharm.2014.11.003>.
- [2] A.C. Rossman, The physiology of the nicotinic acetylcholine receptor and its importance in the administration of anesthesia, *AANA journal* 79 (2011). PMID: 23256274.
- [3] G. Sharma, S. Vijayaraghavan, Nicotinic receptors: role in addiction and other disorders of the brain, *Subst. Abuse Res. Treat.* 1 (2008), <https://doi.org/10.1177/117822180800100005>, 117822180800100005.
- [4] T.J. Davis, Alcohol's actions on neuronal nicotinic acetylcholine receptors, *Alcohol Res. Health* 29 (2006) 179–185. PMID: 17373406.
- [5] Y. Tian, J.R. Gunther, I.H. Liao, D. Liu, B.P. Ander, B.S. Stamova, L. Lit, G. C. Jickling, H. Xu, X. Zhan, GABA-and acetylcholine-related gene expression in blood correlate with tic severity and microarray evidence for alternative splicing in Tourette syndrome: a pilot study, *Brain Res.* 1381 (2011) 228–236, <https://doi.org/10.1016/j.brainres.2011.01.026>.
- [6] T.E. Wilens, M.W. Decker, Neuronal nicotinic receptor agonists for the treatment of attention-deficit/hyperactivity disorder: focus on cognition, *Biochem. Pharmacol.* 74 (2007) 1212–1223, <https://doi.org/10.1016/j.bcp.2007.07.002>.
- [7] M. Ray, A. Graham, M. Lee, R. Perry, J. Court, E. Perry, Neuronal nicotinic acetylcholine receptor subunits in autism: an immunohistochemical investigation in the thalamus, *Neurobiol. Dis.* 19 (2005) 366–377, <https://doi.org/10.1016/j.nbd.2005.01.017>.
- [8] N.S. Philip, L.L. Carpenter, A.R. Tyrka, L.H. Price, Nicotinic acetylcholine receptors and depression: a review of the preclinical and clinical literature, *Psychopharmacology* 212 (2010) 1–12, <https://doi.org/10.1007/s00213-010-1932-6>.
- [9] D. Gangitano, R. Salas, Y. Teng, E. Perez, M. De Biasi, Progesterone modulation of  $\alpha 5$  nAChR subunits influences anxiety-related behavior during estrus cycle, *Gene Brain Behav.* 8 (2009) 398–406, <https://doi.org/10.1111/j.1601-183X.2009.00476.x>.
- [10] P.T. Francis, A.M. Palmer, M. Snape, G.K. Wilcock, The cholinergic hypothesis of Alzheimer's disease: a review of progress, *J. Neurol. Neurosurg. Psychiatr.* 66 (1999) 137–147, <https://doi.org/10.1136/jnnp.66.2.137>.
- [11] L.Y. Ballester, C.M. Capó-Vélez, W.F. García-Beltrán, F.M. Ramos, E. Vázquez-Rosa, R. Ríos, J.R. Mercado, R.I. Meléndez, J.A. Lasalde-Dominicci, Up-regulation of the neuronal nicotinic receptor  $\alpha 7$  by HIV glycoprotein 120 potential implications for HIV-associated neurocognitive disorder, *J. Biol. Chem.* 287 (2012) 3079–3086, <https://doi.org/10.1074/jbc.M111.262543>.
- [12] C.M. Capó-Vélez, B. Morales-Vargas, A. García-González, J.G. Grajales-Reyes, M. Delgado-Vélez, B. Madera, C.A. Báez-Pagán, O. Quesada, J.A. Lasalde-Dominicci, The  $\alpha 7$ -nicotinic receptor contributes to gp120-induced neurotoxicity: implications in HIV-associated neurocognitive disorders, *Sci. Rep.* 8 (2018) 1–11, <https://doi.org/10.1038/s41598-018-20271-x>.
- [13] J.-P. Changeux, The nicotinic acetylcholine receptor: the founding father of the pentameric ligand-gated ion channel superfamily, *J. Biol. Chem.* 287 (2012) 40207–40215, <https://doi.org/10.1074/jbc.R112.407668>.
- [14] P.-J. Corringer, F. Poitevin, M.S. Prevost, L. Sauguet, M. Delarue, J.-P. Changeux, Structure and pharmacology of pentameric receptor channels: from bacteria to brain, *Structure* 20 (2012) 941–956, <https://doi.org/10.1016/j.str.2012.05.003>.
- [15] K. Brejč, W.J. van Dijk, R.V. Klaassen, M. Schuurmans, J. van der Oost, A.B. Smit, T.K. Sixma, Crystal structure of an ACh-binding protein reveals the ligand-binding domain of nicotinic receptors, *Nature* 411 (2001) 269–276, <https://doi.org/10.1038/35077011>.

- [16] P.H. Celie, S.E. van Rossum-Fikkert, W.J. van Dijk, K. Brejc, A.B. Smit, T.K. Sixma, Nicotine and carbamylcholine binding to nicotinic acetylcholine receptors as studied in AChBP crystal structures, *Neuron* 41 (2004) 907–914, [https://doi.org/10.1016/S0896-6273\(04\)00115-1](https://doi.org/10.1016/S0896-6273(04)00115-1).
- [17] S.B. Hansen, G. Sulzenbacher, T. Huxford, P. Marchot, P. Taylor, Y. Bourne, Structures of *Aplysia* AChBP complexes with nicotinic agonists and antagonists reveal distinctive binding interfaces and conformations, *EMBO J.* 24 (2005) 3635–3646, <https://doi.org/10.1038/sj.emboj.7600828>.
- [18] X. Huang, H. Chen, K. Michelsen, S. Schneider, P.L. Shaffer, Crystal structure of human glycine receptor  $\alpha 3$  bound to antagonist strychnine, *Nature* 526 (2015) 277–280, <https://doi.org/10.1038/nature14972>.
- [19] F. Pfeiffer, D. Graham, H. Betz, Purification by affinity chromatography of the glycine receptor of rat spinal cord, *J. Biol. Chem.* 257 (1982) 9389–9393. PMID: 6286620.
- [20] X. Huang, P.L. Shaffer, S. Ayube, H. Bregman, H. Chen, S.G. Lehto, J.A. Luther, D. J. Matson, S.I. McDonough, K. Michelsen, Crystal structures of human glycine receptor  $\alpha 3$  bound to a novel class of analgesic potentiators, *Nat. Struct. Mol. Biol.* 24 (2017) 108, <https://doi.org/10.1038/nsmb.3329>.
- [21] P.R. Schofield, M.G. Darlison, N. Fujita, D.R. Burt, F.A. Stephenson, H. Rodriguez, L.M. Rhee, J. Ramachandran, V. Reale, T.A. Glencorse, Sequence and functional expression of the GABA A receptor shows a ligand-gated receptor super-family, *Nature* 328 (1987) 221–227, <https://doi.org/10.1038/328221a0>.
- [22] P.S. Miller, A.R. Aricescu, Crystal structure of a human GABA A receptor, *Nature* 512 (2014) 270–275, <https://doi.org/10.1038/nature13293>.
- [23] G. Hassaine, C. Deluz, L. Grasso, R. Wyss, M.B. Tol, R. Hovius, A. Graff, H. Stahlberg, T. Tomizaki, A. Desmyter, X-ray structure of the mouse serotonin 5-HT 3 receptor, *Nature* 512 (2014) 276–281, <https://doi.org/10.1038/nature13552>.
- [24] S. Basak, Y. Gicheru, A. Samanta, S.K. Molugu, W. Huang, M. la de Fuente, T. Hughes, D.J. Taylor, M.T. Nieman, V. Moiseenkova-Bell, Cryo-EM structure of 5-HT 3A receptor in its resting conformation, *Nat. Commun.* 9 (2018) 1–10, <https://doi.org/10.1038/s41467-018-02997-4>.
- [25] R.J. Hilf, R. Dutzler, X-ray structure of a prokaryotic pentameric ligand-gated ion channel, *Nature* 452 (2008) 375–379, <https://doi.org/10.1038/nature07461>.
- [26] R.J. Hilf, R. Dutzler, Structure of a potentially open state of a proton-activated pentameric ligand-gated ion channel, *Nature* 457 (2009) 115–118, <https://doi.org/10.1038/nature07461>.
- [27] L. Sauguet, F. Poitevin, S. Murail, C. Van Renterghem, G. Moraga-Cid, L. Malherbe, A.W. Thompson, P. Koehl, P.J. Corringer, M. Baaden, Structural basis for ion permeation mechanism in pentameric ligand-gated ion channels, *EMBO J.* 32 (2013) 728–741, <https://doi.org/10.1038/emboj.2013.17>.
- [28] J.B. Cohen, M. Weber, M. Huchet, J.-P. Changeux, Purification from Torpedo marmorata electric tissue of membrane fragments particularly rich in cholinergic receptor protein, *FEBS Lett.* 26 (1972) 43–47, [https://doi.org/10.1016/0014-5793\(72\)80538-6](https://doi.org/10.1016/0014-5793(72)80538-6).
- [29] C. Toyoshima, N. Unwin, Ion channel of acetylcholine receptor reconstructed from images of postsynaptic membranes, *Nature* 336 (1988) 247–250, <https://doi.org/10.1038/336247a0>.
- [30] N. Unwin, Nicotinic acetylcholine receptor at 9 resolution, *J. Mol. Biol.* 229 (1993), 1101–1101, <https://www.DOI:10.1006/jmbi.1993.1107>.
- [31] A. Miyazawa, Y. Fujiyoshi, M. Stowell, N. Unwin, Nicotinic acetylcholine receptor at 4.6 Å resolution: transverse tunnels in the channel, *J. Mol. Biol.* 288 (1999) 765–786, <https://doi.org/10.1006/jmbi.1999.2721>.
- [32] N. Unwin, Refined structure of the nicotinic acetylcholine receptor at 4 Å resolution, *J. Mol. Biol.* 346 (2005) 967–989, <https://doi.org/10.1016/j.jmb.2004.12.031>.
- [33] M.M. Rahman, J. Teng, B.T. Worrell, C.M. Novello, M. Lee, A. Karlin, M. H. Stowell, R.E. Hibbs, Structure of the native muscle-type nicotinic receptor and inhibition by snake venom toxins, *Neuron* (2020), <https://doi.org/10.1016/j.neuron.2020.03.012>.
- [34] C.L. Morales-Perez, C.M. Novello, R.E. Hibbs, X-ray structure of the human  $\alpha 4\beta 2$  nicotinic receptor, *Nature* 538 (2016) 411–415, <https://doi.org/10.1038/nature19785>.
- [35] S. Edelstein, W.B. Beyer, A. Elderfrawi, M. Elderfrawi, Molecular weight of the acetylcholine receptors of electric organs and the effect of Triton X-100, *J. Biol. Chem.* 250 (1975) 6101–6106. PMID: 1150674.
- [36] T. Grutter, S. Bertrand, F. Kotzyba-Hibert, D. Bertrand, M. Goeldner, Structural reorganization of the acetylcholine binding site of the Torpedo nicotinic receptor as revealed by dynamic photoaffinity labeling, *ChemBiochem* 3 (2002) 652–658, [https://doi.org/10.1002/1439-7633\(20020703\)3:7<652::AID-CBIC652>3.0.CO;2-L](https://doi.org/10.1002/1439-7633(20020703)3:7<652::AID-CBIC652>3.0.CO;2-L).
- [37] F.J. Barrantes, G. Mieskes, T. Wallimann, A membrane-associated creatine kinase (EC 2.7. 3.2) identified as an acidic species of the non-receptor, peripheral v-proteins in Torpedo acetylcholine receptor membranes, *FEBS Lett.* 152 (1983) 270–276, [https://doi.org/10.1016/0014-5793\(83\)80394-9](https://doi.org/10.1016/0014-5793(83)80394-9).
- [38] F. Hucho, G. Bandini, B.A. Suárez-Isla, The acetylcholine receptor as part of a protein complex in receptor-enriched membrane fragments from Torpedo californica electric tissue, *Eur. J. Biochem.* 83 (1978) 335–340, <https://doi.org/10.1111/j.1432-1033.1978.tb12099.x>.
- [39] L.F. Padilla-Morales, J.O. Colón-Sáez, J.E. González-Nieves, O. Quesada-González, J.A. Lasalde-Dominicci, Assessment of the functionality and stability of detergent purified nAChR from Torpedo using lipidic matrixes and macroscopic electrophysiology, *Biochim. Biophys. Acta Biomembr.* 1858 (2016) 47–56, <https://doi.org/10.1016/j.bbmembr.2015.10.002>.
- [40] L.F. Padilla-Morales, J.O. Colón-Sáez, J.E. González-Nieves, O. Quesada-González, J.A. Lasalde-Dominicci, Functionality and stability data of detergent purified nAChR from Torpedo using lipidic matrixes and macroscopic electrophysiology, *Data in brief* 6 (2016) 433–437, <https://doi.org/10.1016/j.dib.2015.12.010>.
- [41] O. Quesada, C. González-Freire, M.C. Ferrer, J.O. Colón-Sáez, E. Fernández-García, J. Mercado, A. Dávila, R. Morales, J.A. Lasalde-Dominicci, Uncovering the lipidic basis for the preparation of functional nicotinic acetylcholine receptor detergent complexes for structural studies, *Sci. Rep.* 6 (2016) 32766, <https://doi.org/10.1038/srep32766>.
- [42] G.A. Asmar-Rovira, A.M. Asseo-García, O. Quesada, M.A. Hanson, A. Cheng, C. Noguera, J.A. Lasalde-Dominicci, R.C. Stevens, Biophysical and ion channel functional characterization of the Torpedo californica nicotinic acetylcholine receptor in varying detergent–lipid environments, *J. Membr. Biol.* 223 (2008) 13–26, <https://doi.org/10.1007/s00232-008-9107-7>.
- [43] S.E. Mate, A. Lersong, K. Brown, E. Hoffman, Integrated Genomics/proteomics of the Torpedo californica Electric Organ to Assess Concordance with the Mammalian Neuromuscular Junction (NMJ) Proteome and to Identify Novel Proteins, *Federation of American Societies for Experimental Biology*, 2011.
- [44] M.A. Bowe, K.A. Deyst, J.D. Leszyk, J.R. Fallon, Identification and purification of an agrin receptor from Torpedo postsynaptic membranes: a heteromeric complex related to the dystroglycans, *Neuron* 12 (1994) 1173–1180, [https://doi.org/10.1016/0896-6273\(94\)90324-7](https://doi.org/10.1016/0896-6273(94)90324-7).
- [45] K.R. Wagner, J.B. Cohen, R.L. Haganir, The 87K postsynaptic membrane protein from Torpedo is a protein-tyrosine kinase substrate homologous to dystrophin, *Neuron* 10 (1993) 511–522, [https://doi.org/10.1016/0896-6273\(93\)90338-R](https://doi.org/10.1016/0896-6273(93)90338-R).
- [46] C. Carr, D. McCourt, J.B. Cohen, The 43 kilodalton protein of Torpedo nicotinic postsynaptic membranes: purification and determination of primary structure, *Biochemistry* 26 (1987) 7090–7102, <https://doi.org/10.1021/bi00396a034>.
- [47] B.M. Conti-Tronconi, S. Dunn, E.A. Barnard, J.O. Dolly, F.A. Lai, N. Ray, M. A. Raftery, Brain and muscle nicotinic acetylcholine receptors are different but homologous proteins, *Proc. Natl. Acad. Sci. Unit. States Am.* 82 (1985) 5208–5212, <https://doi.org/10.1073/pnas.82.15.5208>.
- [48] J. Lindstrom, B. Walter, B. Einarson, Immunological similarities between subunits of acetylcholine receptors from Torpedo, Electrophorus, and mammalian muscle, *Biochemistry* 18 (1979) 4470–4480, <https://doi.org/10.1021/bi00588a004>.
- [49] M. Raftery, R. Vandlen, D. Michaelson, J. Bode, T. Moody, Y. Chao, K. Reed, J. Deusch, J. Duguid, The biochemistry of an acetylcholine receptor, *J. Supramol. Struct.* 2 (1974) 582–592, <https://doi.org/10.1002/jss.400020506>.
- [50] T. Saitoh, R. Oswald, L.P. Wonnego, J.-P. Changeux, Conditions for the selective labelling of the 66 000 dalton chain of the acetylcholine receptor by the covalent non-competitive blocker 5-azido-[3H] trimethisquin, *FEBS Lett.* 116 (1980) 30–36, [https://doi.org/10.1016/0014-5793\(80\)80522-9](https://doi.org/10.1016/0014-5793(80)80522-9).
- [51] C.L. Weill, M.G. McNamee, A. Karlin, Affinity-labeling of purified acetylcholine receptor from Torpedo californica, *Biochem. Biophys. Res. Commun.* 61 (1974) 997–1003, [https://doi.org/10.1016/0006-291X\(74\)90254-X](https://doi.org/10.1016/0006-291X(74)90254-X).
- [52] E. Kubalek, S. Ralston, J. Lindstrom, N. Unwin, Location of subunits within the acetylcholine receptor by electron image analysis of tubular crystals from Torpedo marmorata, *J. Cell Biol.* 105 (1987) 9–18, <https://doi.org/10.1083/jcb.105.1.9>.
- [53] A. Miyazawa, Y. Fujiyoshi, N. Unwin, Structure and gating mechanism of the acetylcholine receptor pore, *Nature* 423 (2003) 949–955, <https://doi.org/10.1038/nature01748>.
- [54] N. Unwin, Segregation of lipids near acetylcholine-receptor channels imaged by cryo-EM, *IUCr J.* 4 (2017) 393–399, <https://doi.org/10.1107/S2052252517005243>.
- [55] I. Tsigelny, N. Sugiyama, S.M. Sine, P. Taylor, A model of the nicotinic receptor extracellular domain based on sequence identity and residue location, *Biophys. J.* 73 (1997) 52–66, [https://doi.org/10.1016/S0006-3495\(97\)78047-0](https://doi.org/10.1016/S0006-3495(97)78047-0).
- [56] O.T. Jones, M.G. McNamee, Annular and nonannular binding sites for cholesterol associated with the nicotinic acetylcholine receptor, *Biochemistry* 27 (1988) 2364–2374, <https://doi.org/10.1021/bi00407a018>.
- [57] A. Bhushan, M.G. McNamee, Correlation of phospholipid structure with functional effects on the nicotinic acetylcholine receptor. A modulatory role for phosphatidic acid, *Biophys. J.* 64 (1993) 716–723, [https://doi.org/10.1016/S0006-3495\(93\)81431-0](https://doi.org/10.1016/S0006-3495(93)81431-0).
- [58] J.A. Lasalde, S. Tamamizu, D.H. Butler, C.R.T. Vibat, B. Hung, M.G. McNamee, Tryptophan substitutions at the lipid-exposed transmembrane segment M4 of Torpedo californica acetylcholine receptor govern channel gating, *Biochemistry* 35 (1996) 14139–14148, <https://doi.org/10.1021/bi961583l>.
- [59] H.R. Arias, The high-affinity quinacrine binding site is located at a non-annular lipid domain of the nicotinic acetylcholine receptor, *Biochim. Biophys. Acta Lipids Lipid. Metabol.* 1347 (1997) 9–22, [https://doi.org/10.1016/S0005-2760\(97\)00045-3](https://doi.org/10.1016/S0005-2760(97)00045-3).
- [60] F.J. Barrantes, Lipid matters: nicotinic acetylcholine receptor–lipid interactions, *Mol. Membr. Biol.* 19 (2002) 277–284, <https://doi.org/10.1080/09687680210166226>.
- [61] F. Barrantes, Structural basis for lipid modulation of nicotinic acetylcholine receptor function, *Brain Res. Rev.* 47 (2004) 71–95, <https://doi.org/10.1016/j.brainresrev.2004.06.008>.
- [62] J.L. Popot, R.A. Demel, A. Sobel, L.L. Van Deenen, J.P. Changeux, Interaction of the acetylcholine (nicotinic) receptor protein from Torpedo marmorata electric organ with monolayers of pure lipids, *Eur. J. Biochem.* 85 (1978) 27–42, <https://doi.org/10.1111/j.1432-1033.1978.tb12209.x>.
- [63] T.M. Fong, M.G. McNamee, Stabilization of acetylcholine receptor secondary structure by cholesterol and negatively charged phospholipids in membranes, *Biochemistry* 26 (1987) 3871–3880, <https://doi.org/10.1021/bi00387a020>.

- [64] M. Criado, H. Eibl, F. Barrantes, Functional properties of the acetylcholine receptor incorporated in model lipid membranes. Differential effects of chain length and head group of phospholipids on receptor affinity states and receptor-mediated ion translocation, *J. Biol. Chem.* 259 (1984) 9188–9198. PMID: 6746645.
- [65] M. McCarthy, M.A. Moore, Effects of lipids and detergents on the conformation of the nicotinic acetylcholine receptor from *Torpedo californica*, *J. Biol. Chem.* 267 (1992) 7655–7663. PMID: 1560000.
- [66] N. Methot, C.N. Demers, J.E. Baenziger, Structure of both the ligand- and lipid-dependent channel-inactive states of the nicotinic acetylcholine receptor probed by FTIR spectroscopy and hydrogen exchange, *Biochemistry* 34 (1995) 15142–15149. <https://doi.org/10.1021/bi00046a021>.
- [67] S.E. Ryan, C.N. Demers, J.P. Chew, J.E. Baenziger, Structural effects of neutral and anionic lipids on the nicotinic acetylcholine receptor an infrared difference spectroscopy study, *J. Biol. Chem.* 271 (1996) 24590–24597. <https://doi.org/10.1074/jbc.271.40.24590>.
- [68] C. Gallegos, M. Pediconi, F. Barrantes, Ceramides modulate cell-surface acetylcholine receptor levels, *Biochim. Biophys. Acta Biomembr.* 1778 (2008) 917–930. <https://doi.org/10.1016/j.bbame.2007.10.019>.
- [69] J. Corrie, J.E. Baenziger, A lipid-dependent uncoupled conformation of the acetylcholine receptor, *J. Biol. Chem.* 284 (2009) 17819–17825. <https://doi.org/10.1074/jbc.M900030200>.
- [70] X. Cang, Y. Du, Y. Mao, Y. Wang, H. Yang, H. Jiang, Mapping the functional binding sites of cholesterol in  $\beta$ 2-adrenergic receptor by long-time molecular dynamics simulations, *J. Phys. Chem. B* 117 (2013) 1085–1094. <https://doi.org/10.1021/jp3118192>.
- [71] T.M. Fong, M.G. McNamee, Correlation between acetylcholine receptor function and structural properties of membranes, *Biochemistry* 25 (1986) 830–840. <https://doi.org/10.1021/bi00352a015>.
- [72] C. Sunshine, M.G. McNamee, Lipid modulation of nicotinic acetylcholine receptor function: the role of neutral and negatively charged lipids, *Biochim. Biophys. Acta Biomembr.* 1108 (1992) 240–246. [https://doi.org/10.1016/0005-2736\(92\)90031-G](https://doi.org/10.1016/0005-2736(92)90031-G).
- [73] V. Narayanaswami, M.G. McNamee, Protein-lipid interactions and *Torpedo californica* nicotinic acetylcholine receptor function. 2. Membrane fluidity and ligand-mediated alteration in the accessibility of gamma. subunit cysteine residues to cholesterol, *Biochemistry* 32 (1993) 12420–12427. <https://doi.org/10.1021/bi00097a021>.
- [74] S.E. Rankin, G.H. Addona, M.A. Kloczewiak, B. Bugge, K.W. Miller, The cholesterol dependence of activation and fast desensitization of the nicotinic acetylcholine receptor, *Biophys. J.* 73 (1997) 2446–2455. [https://doi.org/10.1016/S0006-3495\(97\)78273-0](https://doi.org/10.1016/S0006-3495(97)78273-0).
- [75] J. Santiago, G.R. Guzmán, L.V. Rojas, R. Marti, G.A. Asmar-Rovira, L.F. Santana, M. McNamee, J.A. Lasalde-Dominicci, Probing the effects of membrane cholesterol in the *Torpedo californica* acetylcholine receptor and the novel lipid-exposed mutation  $\alpha$ C418W in *Xenopus* oocytes, *J. Biol. Chem.* 276 (2001) 46523–46532. <https://doi.org/10.1074/jbc.M104563200>.
- [76] J. Corrie, A.A. Ogrel, E.A. McCarty, M.P. Blanton, J.E. Baenziger, Lipid-protein interactions at the nicotinic acetylcholine receptor A functional coupling between nicotinic receptors and phosphatidic acid-containing lipid bilayers, *J. Biol. Chem.* 277 (2002) 201–208. <https://doi.org/10.1074/jbc.M108341200>.
- [77] A.K. Hamouda, D.C. Chiara, D. Sauls, J.B. Cohen, M.P. Blanton, Cholesterol interacts with transmembrane  $\alpha$ -helices M1, M3, and M4 of the *Torpedo* nicotinic acetylcholine receptor: photolabeling studies using [3H] azicholesterol, *Biochemistry* 45 (2006) 976–986. <https://doi.org/10.1021/bi051978h>.
- [78] C.A. Báez-Pagán, N. del Hoyo-Rivera, O. Quesada, J.D. Otero-Cruz, J.A. Lasalde-Dominicci, Heterogeneous inhibition in macroscopic current responses of four nicotinic acetylcholine receptor subtypes by cholesterol enrichment, *J. Membr. Biol.* 249 (2016) 539–549. <https://doi.org/10.1007/s00232-016-9896-z>.
- [79] J. Fantini, F.J. Barrantes, Sphingolipid/cholesterol regulation of neurotransmitter receptor conformation and function, *Biochim. Biophys. Acta Biomembr.* 1788 (2009) 2345–2361. <https://doi.org/10.1016/j.bbame.2009.08.016>.
- [80] J. Fantini, C. Di Scala, C.J. Baier, F.J. Barrantes, Molecular mechanisms of protein-cholesterol interactions in plasma membranes: functional distinction between topological (tilted) and consensus (CARC/CRAC) domains, *Chem. Phys. Lipids* 199 (2016) 52–60. <https://doi.org/10.1016/j.chemphyslip.2016.02.009>.
- [81] L.F. Padilla-Morales, C.L. Morales-Pérez, C. Pamela, G. Asmar-Rovira, C.A. Báez-Pagán, O. Quesada, J.A. Lasalde-Dominicci, Effects of lipid-analog detergent solubilization on the functionality and lipidic cubic phase mobility of the *Torpedo californica* nicotinic acetylcholine receptor, *J. Membr. Biol.* 243 (2011) 47. <https://doi.org/10.1007/s00232-011-9392-4>.
- [82] V. Cherezov, J. Liu, M. Griffith, M.A. Hanson, R.C. Stevens, LCP-FRAP assay for pre-screening membrane proteins for in meso crystallization, *Cryst. Growth Des.* 8 (2008) 4307–4315. <https://doi.org/10.1021/cg800778j>.
- [83] C. Wenz, M. Marchetti-Deschmann, E. Herwig, E. Schröttner, G. Allmaier, L. Trojer, M. Vollmer, A. Rüfer, A fluorescent derivatization method of proteins for the detection of low-level impurities by microchip capillary gel electrophoresis, *Electrophoresis* 31 (2010) 611–617. <https://doi.org/10.1002/elps.200900346>.
- [84] V.U.W. Nicole Engel, Martina Marchetti-Deschmann, and Günter Allmaier, *A Comparative Study of Analytical Parameters for Proteins with Different Degrees of Glycosylation*, Agilent Technologies, Inc., 2016, 5991-593435EN.
- [85] Agilent High Sensitivity Protein 250 Kit Guide, Agilent Technologies Manual, Reference Number G2938-90310, Rev. B, Agilent Technologies, Inc., 2016.
- [86] L. Bousse, S. Mouradian, A. Minalla, H. Yee, K. Williams, R. Dubrow, Protein sizing on a microchip, *Anal. Chem.* 73 (2001) 1207–1212. <https://doi.org/10.1021/ac0012492>.
- [87] A. Rüfer, Therapeutic protein analysis with the Agilent 2100 bioanalyzer, *Biotechniques* 49 (2010) 669–671. <https://doi.org/10.2144/000113500>.
- [88] C. Wenz, A. Rüfer, Immunoprecipitation and the high sensitivity protein 250 assay, *Biotechniques* 48 (2010) 330–332. <https://doi.org/10.2144/000113404>.
- [89] B.S. Antharavally, K.A. Mallia, M.M. Rosenblatt, A.M. Salunkhe, J.C. Rogers, P. Haney, N. Haghdost, Efficient removal of detergents from proteins and peptides in a spin column format, *Anal. Biochem.* 416 (2011) 39–44. <https://doi.org/10.1016/j.ab.2011.05.013>.
- [90] J. Marsal, G. Tigyí, R. Miledí, Incorporation of acetylcholine receptors and Cl<sup>-</sup> channels in *Xenopus* oocytes injected with *Torpedo* electroplaque membranes, *Proc. Natl. Acad. Sci. Unit. States Am.* 92 (1995) 5224–5228. <https://doi.org/10.1073/pnas.92.11.5224>.
- [91] A. Bhushan, M.G. McNamee, Differential scanning calorimetry and Fourier transform infrared analysis of lipid-protein interactions involving the nicotinic acetylcholine receptor, *Biochim. Biophys. Acta Biomembr.* 1027 (1990) 93–101. [https://doi.org/10.1016/0005-2736\(90\)90053-Q](https://doi.org/10.1016/0005-2736(90)90053-Q).
- [92] E.L. Ochoa, A.W. Dalziel, M.G. McNamee, Reconstitution of acetylcholine receptor function in lipid vesicles of defined composition, *Biochim. Biophys. Acta Biomembr.* 727 (1983) 151–162. [https://doi.org/10.1016/0005-2736\(83\)90379-6](https://doi.org/10.1016/0005-2736(83)90379-6).
- [93] R. Maldonado-Hernández, O. Quesada, J.A. Lasalde-Dominicci, Biophysical Characterization dataset of native nicotinic acetylcholine receptor in lipid-like detergent complexes, 2020. <https://doi.org/10.1016/j.dib.2020.106230>. Data in Brief.
- [94] R.G. Frost, J.F. Monthony, S.C. Engelhorn, C.J. Siebert, Covalent immobilization of proteins to N-hydroxysuccinimide ester derivatives of agarose: effect of protein charge on immobilization, *Biochim. Biophys. Acta Protein Struct.* 670 (1981) 163–169. [https://doi.org/10.1016/0005-2795\(81\)90004-0](https://doi.org/10.1016/0005-2795(81)90004-0).
- [95] R. Anholt, J. Lindstrom, M. Montal, Functional equivalence of monomeric and dimeric forms of purified acetylcholine receptors from *Torpedo californica* in reconstituted lipid vesicles, *Eur. J. Biochem.* 109 (1980) 481–487. <https://doi.org/10.1111/j.1432-1033.1980.tb04819.x>.
- [96] A. Sobel, M. Weber, J.P. Changeux, Large-scale purification of the acetylcholine-receptor protein in its membrane-bound and detergent-extracted forms from *Torpedo marmorata* electric organ, *Eur. J. Biochem.* 80 (1977) 215–224. <https://doi.org/10.1111/j.1432-1033.1977.tb11874.x>.
- [97] M. Criado, H. Eibl, F. Barrantes, Effects of lipids on acetylcholine receptor. Essential need of cholesterol for maintenance of agonist-induced state transitions in lipid vesicles, *Biochemistry* 21 (1982) 3622–3629. <https://doi.org/10.1021/bi00258a015>.
- [98] G. Fernandez-Ballester, J. Castresana, A.M. Fernandez, J.-L.R. Arrondo, J. A. Ferragut, J.M. Gonzalez-Ros, A role for cholesterol as a structural effector of the nicotinic acetylcholine receptor, *Biochemistry* 33 (1994) 4065–4071. <https://doi.org/10.1021/bi00179a035>.
- [99] K. Burger, G. Gimpl, F. Fahrenholz, Regulation of receptor function by cholesterol, *Cellular and Molecular Life Sciences CMLS* 57 (2000) 1577–1592. <https://doi.org/10.1007/PL00000643>.
- [100] G. Brannigan, J. Hénin, R. Law, R. Eckenhoff, M.L. Klein, Embedded cholesterol in the nicotinic acetylcholine receptor, *Proc. Natl. Acad. Sci. Unit. States Am.* 105 (2008) 14418–14423. <https://doi.org/10.1073/pnas.0803029105>.
- [101] A.K. Hamouda, D.C. Chiara, M.P. Blanton, J.B. Cohen, Probing the structure of the affinity-purified and lipid-reconstituted *Torpedo* nicotinic acetylcholine receptor, *Biochemistry* 47 (2008) 12787–12794. <https://doi.org/10.1021/bi801476j>.
- [102] P. Ontong, Y. Hatada, S.i. Taniguchi, I. Kakizaki, N. Itano, Effect of a cholesterol-rich lipid environment on the enzymatic activity of reconstituted hyaluronan synthase, *Biochem. Biophys. Res. Commun.* 443 (2014) 666–671. <https://doi.org/10.1016/j.bbrc.2013.12.028>.
- [103] J.E. Baenziger, J.A. Domville, J.D. Therien, The role of cholesterol in the activation of nicotinic acetylcholine receptors, *Curr. Top. Membr.* (2017) 95–137. Elsevier.
- [104] J. Grouleff, S.J. Irudayam, K.K. Skeby, B. Schiøtt, The influence of cholesterol on membrane protein structure, function, and dynamics studied by molecular dynamics simulations, *Biochim. Biophys. Acta Biomembr.* 1848 (2015) 1783–1795. <https://doi.org/10.1016/j.bbame.2015.03.029>.
- [105] M.-B. Lascombe, M. Ponchet, P. Venard, M.-L. Milat, J.-P. Blein, T. Prangé, The 1.45 Å resolution structure of the cryptogem-cholesterol complex: a close-up view of a sterol carrier protein (SCP) active site, *Acta Crystallogr. Sect. D Biol. Crystallogr.* 58 (2002) 1442–1447. <https://doi.org/10.1107/S0907444902011745>.
- [106] V. Cherezov, D.M. Rosenbaum, M.A. Hanson, S.G. Rasmussen, F.S. Thian, T. S. Kobilka, H.-J. Choi, P. Kuhn, W.I. Weis, B.K. Kobilka, High-resolution crystal structure of an engineered human  $\beta$ 2-adrenergic G protein-coupled receptor, *Science* 318 (2007) 1258–1265. <https://doi.org/10.1126/science.1150577>.
- [107] A. Gharpure, J. Teng, Y. Zhuang, C.M. Novello, R.M. Walsh Jr., R. Cabuco, R. J. Howard, N.T. Zaveri, E. Lindahl, R.E. Hibbs, Agonist selectivity and ion permeation in the  $\alpha$ 3 $\beta$ 4 ganglionic nicotinic receptor, *Neuron* 104 (2019) 501–511. <https://doi.org/10.1016/j.neuron.2019.07.030>, e506.
- [108] V. Cherezov, Lipidic cubic phase technologies for membrane protein structural studies, *Curr. Opin. Struct. Biol.* 21 (2011) 559–566. <https://doi.org/10.1016/j.sbi.2011.06.007>.
- [109] W. Liu, V. Cherezov, Crystallization of membrane proteins in lipidic mesophases, *JoVE* (2011), e2501. <https://doi.org/10.3791/2501>.

- [110] F. Xu, W. Liu, M.A. Hanson, R.C. Stevens, V. Cherezov, Development of an automated high throughput LCP-FRAP assay to guide membrane protein crystallization in lipid mesophases, *Cryst. Growth Des.* 11 (2011) 1193–1201, <https://doi.org/10.1021/cg101385e>.
- [111] E.M. Landau, J.P. Rosenbusch, Lipidic cubic phases: a novel concept for the crystallization of membrane proteins, *Proc. Natl. Acad. Sci. Unit. States Am.* 93 (1996) 14532–14535, <https://doi.org/10.1073/pnas.93.25.14532>.
- [112] H. Li, V. Papadopoulos, Peripheral-type benzodiazepine receptor function in cholesterol transport. Identification of a putative cholesterol recognition/interaction amino acid sequence and consensus pattern, *Endocrinology* 139 (1998) 4991–4997, <https://doi.org/10.1210/endo.139.12.6390>.
- [113] N. Jamin, J.-M. Neumann, M.A. Ostuni, T.K.N. Vu, Z.-X. Yao, S. Murail, J.-C. Robert, C. Giatzakis, V. Papadopoulos, J.-J. Lacapere, Characterization of the cholesterol recognition amino acid consensus sequence of the peripheral-type benzodiazepine receptor, *Mol. Endocrinol.* 19 (2005) 588–594, <https://doi.org/10.1210/me.2004-0308>.
- [114] A.N. Bukiya, A.M. Dopico, Common structural features of cholesterol binding sites in crystallized soluble proteins, *J. Lipid Res.* 58 (2017) 1044–1054, <https://doi.org/10.1194/jlr.R073452>.
- [115] H. Haviv, M. Habeck, R. Kanai, C. Toyoshima, S.J. Karlsh, Neutral phospholipids stimulate Na, K-ATPase activity a specific lipid-protein interaction, *J. Biol. Chem.* 288 (2013) 10073–10081, <https://doi.org/10.1074/jbc.M112.446997>.
- [116] Y. Sonntag, M. Musgaard, C. Olesen, B. Schiøtt, J.V. Møller, P. Nissen, L. Thøgersen, Mutual adaptation of a membrane protein and its lipid bilayer during conformational changes, *Nat. Commun.* 2 (2011) 1–7, <https://doi.org/10.1038/ncomms1307>.
- [117] C. Koshy, E.S. Schweikhard, R.M. Gärtner, C. Perez, Ö. Yildiz, C. Ziegler, Structural evidence for functional lipid interactions in the betaine transporter BetP, *EMBO J.* 32 (2013) 3096–3105, <https://doi.org/10.1038/emboj.2013.226>.
- [118] S. Mehmood, V. Corradi, H.G. Choudhury, R. Hussain, P. Becker, D. Axford, S. Zirah, S. Rebuffat, D.P. Tieleman, C.V. Robinson, Structural and functional basis for lipid synergy on the activity of the antibacterial peptide ABC transporter McjD, *J. Biol. Chem.* 291 (2016) 21656–21668, <https://doi.org/10.1074/jbc.M116.732107>.
- [119] E. Pyle, A.C. Kalli, S. Amillis, Z. Hall, A.M. Lau, A.C. Hanyaloglu, G. Diallinas, B. Byrne, A. Politis, Structural lipids enable the formation of functional oligomers of the eukaryotic purine symporter UapA, *Cell chemical biology* 25 (2018) 840–848, <https://doi.org/10.1016/j.chembiol.2018.03.011>, e844.
- [120] C. Wang, A. Ralko, Z. Ren, A. Rosenhouse-Dantsker, X. Yang, *Modes of Cholesterol Binding in Membrane Proteins: A Joint Analysis of 73 Crystal Structures, Direct Mechanisms in Cholesterol Modulation of Protein Function*, Springer, 2019, pp. 67–86.
- [121] C.J. Baier, J. Fantini, F.J. Barrantes, Disclosure of cholesterol recognition motifs in transmembrane domains of the human nicotinic acetylcholine receptor, *Sci. Rep.* 1 (2011) 69, <https://doi.org/10.1038/srep00069>.
- [122] C. Di Scala, C.J. Baier, L.S. Evans, P.T. Williams, J. Fantini, F.J. Barrantes, Relevance of CARC and CRAC cholesterol-recognition motifs in the nicotinic acetylcholine receptor and other membrane-bound receptors, *Curr. Top. Membr.* (2017) 3–23. Elsevier.
- [123] X. Zhou, J. Xu, Free cholesterol induces higher  $\beta$ -sheet content in A $\beta$  peptide oligomers by aromatic interaction with Phe19, *PLoS One* 7 (2012), <https://doi.org/10.1371/journal.pone.0046245>.
- [124] Y. Tashima, R. Oe, S. Lee, G. Sugihara, E.J. Chambers, M. Takahashi, T. Yamada, The effect of cholesterol and monosialoganglioside (GM1) on the release and aggregation of amyloid  $\beta$ -peptide from liposomes prepared from brain membrane-like lipids, *J. Biol. Chem.* 279 (2004) 17587–17595, <https://doi.org/10.1074/jbc.M308622000>.
- [125] S. Kumar, C.-J. Tsai, R. Nussinov, Factors enhancing protein thermostability, *Protein Eng.* 13 (2000) 179–191, <https://doi.org/10.1093/protein/13.3.179>.
- [126] S. Schick, L. Chen, E. Li, J. Lin, I. Köper, K. Hristova, Assembly of the M2 tetramer is strongly modulated by lipid chain length, *Biophys. J.* 99 (2010) 1810–1817, <https://doi.org/10.1016/j.bpj.2010.07.026>.
- [127] S.M. Ireland, A. Sula, B.A. Wallace, Thermal melt circular dichroism spectroscopic studies for identifying stabilising amphipathic molecules for the voltage-gated sodium channel NavMs, *Biopolymers* 109 (2018), e23067, <https://doi.org/10.1002/bip.23067>.
- [128] V.V. Khrustalev, T.A. Khrustaleva, K. Szpotkowski, V.V. Poboinev, K. Y. Kakhouskaya, The part of a long beta hairpin from the scrapie form of the human prion protein is reconstructed in the synthetic CC36 protein, *Proteins: Structure, Function, and Bioinformatics* 84 (2016) 1462–1479, <https://doi.org/10.1002/prot.25090>.
- [129] V.V. Khrustalev, T.A. Khrustaleva, V.V. Poboinev, Amino acid content of beta strands and alpha helices depends on their flanking secondary structure elements, *Biosystems* 168 (2018) 45–54, <https://doi.org/10.1016/j.biosystems.2018.04.002>.
- [130] K. Fujiwara, H. Toda, M. Ikeguchi, Dependence of  $\alpha$ -helical and  $\beta$ -sheet amino acid propensities on the overall protein fold type, *BMC Struct. Biol.* 12 (2012) 18, <https://doi.org/10.1186/1472-6807-12-18>.
- [131] W.M. Moore, L.A. Holladay, D. Puett, R.N. Brady, On the conformation of the acetylcholine receptor protein from Torpedo nobiliana, *FEBS Lett.* 45 (1974) 145–149, <https://doi.org/10.1021/bi00190a026>.
- [132] J. Finer-Moore, R.M. Stroud, Amphipathic analysis and possible formation of the ion channel in an acetylcholine receptor, *Proc. Natl. Acad. Sci. Unit. States Am.* 81 (1984) 155–159, <https://doi.org/10.1073/pnas.81.1.155>.
- [133] D.H. Butler, M.G. McNamee, FTIR analysis of nicotinic acetylcholine receptor secondary structure in reconstituted membranes, *Biochim. Biophys. Acta Biomembr.* 1150 (1993) 17–24, [https://doi.org/10.1016/0005-2736\(93\)90116-H](https://doi.org/10.1016/0005-2736(93)90116-H).
- [134] N. Methot, M.P. McCarthy, J.E. Baenziger, Secondary structure of the nicotinic acetylcholine receptor: implications for structural models of a ligand-gated ion channel, *Biochemistry* 33 (1994) 7709–7717, <https://doi.org/10.1021/bi00190a026>.
- [135] G. Fernandez-Ballester, J. Castresana, J. Arrondo, J. Ferragut, J. Gonzalez-Ros, Protein stability and interaction of the nicotinic acetylcholine receptor with cholinergic ligands studied by Fourier-transform infrared spectroscopy, *Biochem. J.* 288 (1992) 421–426, <https://doi.org/10.1042/bj2880421>.
- [136] N. Le Novère, P.-J. Corringer, J.-P. Changeux, Improved secondary structure predictions for a nicotinic receptor subunit: incorporation of solvent accessibility and experimental data into a two-dimensional representation, *Biophys. J.* 76 (1999) 2329–2345, [https://doi.org/10.1016/S0006-3495\(99\)77390-X](https://doi.org/10.1016/S0006-3495(99)77390-X).
- [137] M.H. Cheng, Y. Xu, P. Tang, Anionic lipid and cholesterol interactions with  $\alpha 4\beta 2$  nAChR: insights from MD simulations, *J. Phys. Chem. B* 113 (2009) 6964–6970, <https://doi.org/10.1021/jp900714b>.
- [138] A.K. Hamouda, M. Sanghvi, D. Sauls, T.K. Machu, M.P. Blanton, Assessing the lipid requirements of the Torpedo californica nicotinic acetylcholine receptor, *Biochemistry* 45 (2006) 4327–4337, <https://doi.org/10.1021/bi052281z>.
- [139] G.H. Addona, H. Sandermann Jr., M.A. Kloczewiak, S.S. Husain, K.W. Miller, Where does cholesterol act during activation of the nicotinic acetylcholine receptor? *Biochim. Biophys. Acta Biomembr.* 1370 (1998) 299–309, [https://doi.org/10.1016/S0005-2736\(97\)00280-0](https://doi.org/10.1016/S0005-2736(97)00280-0).
- [140] S. Antollini, F. Barrantes, Disclosure of discrete sites for phospholipid and sterols at the Protein–lipid interface in native acetylcholine receptor-rich membrane, *Biochemistry* 37 (1998) 16653–16662, <https://doi.org/10.1021/bi9808215>.
- [141] J.E. Baenziger, M.-L. Morris, T.E. Darsaut, S.E. Ryan, Effect of membrane lipid composition on the conformational equilibria of the nicotinic acetylcholine receptor, *J. Biol. Chem.* 275 (2000) 777–784, <https://doi.org/10.1074/jbc.275.2.777>.
- [142] M.J. Thompson, J.A. Domville, J.E. Baenziger, The functional role of the  $\alpha$ M4 transmembrane helix in the muscle nicotinic acetylcholine receptor probed through mutagenesis and co-evolutionary analyses, *J. Biol. Chem.* (2020), <https://doi.org/10.1074/jbc.RA120.013751> jbc. RA120. 013751.